

REPORT DOCUMENTATION PAGE		Form Approved OMB NO. 0704-0188	
Public Reporting Burden for this collection of information is estimated to average 1 hour per response, including the time for reviewing instructions, searching existing data sources, gathering and maintaining the data needed, and completing and reviewing the collection of information. Send comment regarding this burden estimate or any other aspect of this collection of information, including suggestions for reducing this burden, to Washington Headquarters Services, Directorate for Information Operations and Reports, 1215 Jefferson Davis Highway, Suite 1204, Arlington VA, 22202-4302, and to the Office of Management and Budget, Paperwork Reduction Project (0704-0188), Washington DC 20503			
1. AGENCY USE ONLY (Leave Blank)	2. REPORT DATE:	3. REPORT TYPE AND DATES COVERED Final Report 9-Jul-2001 - 30-Jun-2006	
4. TITLE AND SUBTITLE Development of Bicarbonate-Activated Peroxide as a Chemical and Biological Warfare Agent Decontaminant		5. FUNDING NUMBERS DAAD190110691	
6. AUTHORS David E. Richardson		8. PERFORMING ORGANIZATION REPORT NUMBER	
7. PERFORMING ORGANIZATION NAMES AND ADDRESSES University of Florida - Gainesville Division of Sponsored Research 219 Grinter Hall Gainesville, FL 32611 -5500			
9. SPONSORING/MONITORING AGENCY NAME(S) AND ADDRESS(ES) University of Florida - Gainesville 339 Weill Hall P.O. Box 116550 Gainesville, FL 32611 - University Research Office P.O. Box 12211 University of Florida - Gainesville Research Triangle Park, NC 27709-2211		10. SPONSORING / MONITORING AGENCY REPORT NUMBER 42546-CH.1	
11. SUPPLEMENTARY NOTES P O Box 116550 Gainesville, FL 32611 - The views, opinions and/or findings contained in this report are those of the author(s) and should not be construed as an official Department of the Army position, policy or decision, unless so designated by other documentation.			
12. DISTRIBUTION AVAILABILITY STATEMENT Approved for Public Release; Distribution Unlimited		12b. DISTRIBUTION CODE	
13. ABSTRACT (Maximum 200 words) The abstract is below since many authors do not follow the 200 word limit			
14. SUBJECT TERMS decontamination, peroxydicarbonate, peroxide, oxidation, carbon dioxide		15. NUMBER OF PAGES Unknown due to possible attachments	
		16. PRICE CODE	
17. SECURITY CLASSIFICATION OF REPORT UNCLASSIFIED	18. SECURITY CLASSIFICATION ON THIS PAGE UNCLASSIFIED	19. SECURITY CLASSIFICATION OF ABSTRACT UNCLASSIFIED	20. LIMITATION OF ABSTRACT UL

Report Title

FINAL REPORT - Development of Bicarbonate-Activated Peroxide as a Chemical and Biological Warfare Agent Decontaminant

ABSTRACT

Several projects were completed in the development of bicarbonate-activated peroxide (BAP) and other chemistry for the decontamination of chemical and biological warfare agents. The mechanism of formation of the active oxidant, peroxydicarbonate, has been investigated in detail. New surfactants (oxidative surfactant formulations) have been explored. The Mn-catalyzed oxidations by BAP solutions have been investigated to define the active oxidant species in kinetic studies. Initial investigations into new methods for oxidation of chlorite for production of chlorine dioxide have been done. The results to date provide useful insights into various methods for formulating BAP and related oxidative reagents for CWA and BWA applications.

List of papers submitted or published that acknowledge ARO support during this reporting period. List the papers, including journal references, in the following categories:

(a) Papers published in peer-reviewed journals (N/A for none)

Richardson, DE; Regino, CAS; Yao, HR; Johnson, JV. 2003. Methionine oxidation by peroxydicarbonate, a reactive oxygen species formed from CO₂/bicarbonate and hydrogen peroxide. FREE RADICAL BIOLOGY AND MEDICINE 35 (12): 1538-1550.

Yao, HR; Richardson, DE. 2003. Bicarbonate surfactants: Micellar oxidations of aryl sulfides with bicarbonate-activated hydrogen peroxide. JOURNAL OF THE AMERICAN CHEMICAL SOCIETY 125 (20): 6211-6221.

Number of Papers published in peer-reviewed journals: 2.00

(b) Papers published in non-peer-reviewed journals or in conference proceedings (N/A for none)

Number of Papers published in non peer-reviewed journals: 0.00

(c) Presentations

Burke, AP; Richardson, DE. 2004. Oxidation of electrophilic alkenes by bicarbonate-activated peroxide.. ABSTRACTS OF PAPERS OF THE AMERICAN CHEMICAL SOCIETY 228: U795-U795, Part 1.

Denavan, DE; Richardson, DE. 2004. Perhydrolytic cleavage of organophosphates by bicarbonate-activated hydrogen peroxide.. ABSTRACTS OF PAPERS OF THE AMERICAN CHEMICAL SOCIETY 228: U887-U887, Part 1.

Denevan, DE; Richardson, DE. 2003. Bicarbonate-activated hydrogen peroxide in VX simulant decomposition.. ABSTRACTS OF PAPERS OF THE AMERICAN CHEMICAL SOCIETY 225: U95-U95, Part 2.

Ison, A; Weakley, GK; Xu, C; Richardson, DE. 2003. Alkane autoxidation catalyzed by metal diimine coordination complexes.. ABSTRACTS OF PAPERS OF THE AMERICAN CHEMICAL SOCIETY 225: U148-U148, Part 2.

Ison, A; Weakley, GK; Richardson, DE. 2002. Catalytic autoxidation of hydrocarbons using iron-pyridyl coordination complexes.. ABSTRACTS OF PAPERS OF THE AMERICAN CHEMICAL SOCIETY 223: A54-A54, Part 2.

Bennett, DA; Yao, HR; Richardson, DE. 2001. Kinetics and mechanism for the epoxidation of alkenes by peroxydicarbonates.. ABSTRACTS OF PAPERS OF THE AMERICAN CHEMICAL SOCIETY 222: U591-U591, Part 1.

Number of Presentations: 6.00

Non Peer-Reviewed Conference Proceeding publications (other than abstracts):

Number of Non Peer-Reviewed Conference Proceeding publications (other than abstracts): 0

Peer-Reviewed Conference Proceeding publications (other than abstracts):

(d) Manuscripts

Bicarbonate-Catalyzed Hydrogen Peroxide Oxidation of
Cysteine and Related Thiols, Celeste Aida S. Regino and David E. Richardson (submitted, in revision)

The Role of CO₂ in Peroxycarbonate Formation, Yao, H.; Richardson, D. E., (submitted, in revision)

Number of Manuscripts: 2.00

Number of Inventions:**Graduate Students**

<u>NAME</u>	<u>PERCENT SUPPORTED</u>	
Burke, Andrew	1.00	No
Denevan, Daniel	1.00	No
Ison, Ana	0.10	No
Weakley, G. Kenneth	0.10	No
Bennett, Deon	1.00	No
Regino, Celeste	0.50	No
Morgan, Daniel	0.30	No
Mitchell, Michael	0.30	No
FTE Equivalent:	4.30	
Total Number:	8	

Names of Post Doctorates

<u>NAME</u>	<u>PERCENT SUPPORTED</u>	
Ramdon, Dwight	1.00	No
Albert, Ekaterina	0.00	No
Bharathii, Balagam		No
FTE Equivalent:	1.00	
Total Number:	3	

Names of Faculty Supported

<u>NAME</u>	<u>PERCENT SUPPORTED</u>	National Academy Member
David E Richardson	0.00	No
FTE Equivalent:	0.00	
Total Number:	1	

Names of Under Graduate students supported

<u>NAME</u>	<u>PERCENT SUPPORTED</u>
FTE Equivalent:	
Total Number:	

Names of Personnel receiving masters degrees

<u>NAME</u>	
Michael Mitchell	No
Total Number:	1

Names of personnel receiving PhDs

<u>NAME</u>	
Andrew Burke	No
Deon Bennett	No
Celeste Regino	No
Kenneth Weakley	No
Ana Ison	No
Total Number:	5

Names of other research staff

<u>NAME</u>	<u>PERCENT SUPPORTED</u>
FTE Equivalent:	
Total Number:	

Sub Contractors (DD882)

Inventions (DD882)

5 Chlorite Resin for On-Demand Chlorine Dioxide Generation

Patent Filed in US? (5d-1) Y

Patent Filed in Foreign Countries? (5d-2) N

Was the assignment forwarded to the contracting officer? (5e) N

Foreign Countries of application (5g-2):

5a: David E Richardson

5f-1a: University of Florida

5f-c:

Gainesville FL 32611

5a: Dwight C. Ramdon

5f-1a: University of Florida

5f-c:

Gainesville FL 32611

5 On-Demand portable Chlorine Dioxide Generator

Patent Filed in US? (5d-1) Y

Patent Filed in Foreign Countries? (5d-2) N

Was the assignment forwarded to the contracting officer? (5e) N

Foreign Countries of application (5g-2):

5a: David E Richardson

5f-1a: University of Florida

5f-c:

Gainesville FL 32611

5a: Daniel D Denevan

5f-1a: University of Florida

5f-c:

Gainesville FL 32611

Development of Bicarbonate-Activated Peroxide (BAP) as a Chemical and Biological Warfare Agent Decontaminant (42546CH)

David E. Richardson, PI

Department of Chemistry and Center for Catalysis, University of Florida, Gainesville, FL 32605

TABLE OF CONTENTS

I. INTRODUCTION	2
II. FORMATION OF PEROXYMONOCARBONATE AND THE ROLE OF CO₂.....	3
III. ROLE OF TRACE METALS IN STABILITY OF BAP SOLUTIONS	6
IV. INHIBITION OF BAP DISPROPORTIONATION BY COORDINATING ANIONS AND EFFECT OF SOLVENT COMPOSITION	10
V. LIFETIMES OF INHIBITED BAP SOLUTIONS	17
VI. THE ROLE OF THE PEROXYCARBONATE DIANION IN ELECTROPHILIC ALKENE OXIDATION	20
VII. SURFOXIDANTS.....	25
VIII. OXIDATION AND PERHYDROLYSIS OF VX SIMULANTS BY BICARBONATE ACTIVATED PEROXIDE	26
IX. OXIDATION AND PERHYDROLYSIS OF VX SIMULANTS BY HYDROPEROXIDE AND OTHER NUCLEOPHILIC REAGENTS	30
X. N-OXIDATION OF TERTIARY AMINES BY PEROXYMONOCARBONATE: KINETIC AND MECHANISTIC STUDIES	36
XI. BIOLOGICAL IMPLICATIONS OF BAP CHEMISTRY: AMINO ACID, PROTEIN, AND DNA OXIDATION	41
XII. USE OF BAP AS AN ACTIVATOR FOR MN CATALYSTS.....	42
XIII. PRELIMINARY STUDIES ON PORTABLE CHLORINE DIOXIDE GENERATORS.....	43

I. INTRODUCTION

This report summarizes our study of the bicarbonate-activated peroxide oxidation method under grant 42546CH. Oxidative destruction of chemical warfare agents (CWA) and biological warfare agents (BWA) is a common and highly effective approach for decontamination and demilitarization applications. Various oxidizing agents can be used to oxidize sulfides to sulfoxides and sulfones, and some of these have been investigated for simulants related to mustard, HD, and HD itself. In addition, nucleophilic oxidants, such as peroxyanions, can also be used to destroy organophosphate agents, for example VX. We have been investigating the activation of peroxide by the bicarbonate ion as an effective approach to CWA oxidation and perhydrolysis. In addition, we have examined the efficacy of these solutions in destruction of bacteria. The $\text{H}_2\text{O}_2/\text{HCO}_3^-$ reagent combination (or **BAP** for “bicarbonate-activated peroxide”) has several advantages for applications in CWA and BWA decontamination. BAP chemistry is relevant to decontamination solutions in development and/or production, including Decon Green and the original Sandia Foam.

Our results show various approaches that can be used to improve the efficiency of bicarbonate-activated hydrogen peroxide for CWA and BWA destruction. Kinetic and spectroscopic results support the formation of peroxydicarbonate ion (HCO_4^-) as the oxidant in the catalytic oxidation reactions. For perhydrolytic cleavage of organophosphates the peroxydicarbonate dianion (CO_4^{2-}) and hydroperoxide anion (HOO^-) have been shown to be the two primary reactants. Figure 1 shows the labile equilibria between the relevant species for the BAP system. Variation of bicarbonate source, co-solvents, and additives such as surfactants can allow optimization of substrate solubility and reaction rates for applications in chemical warfare agent decontamination.

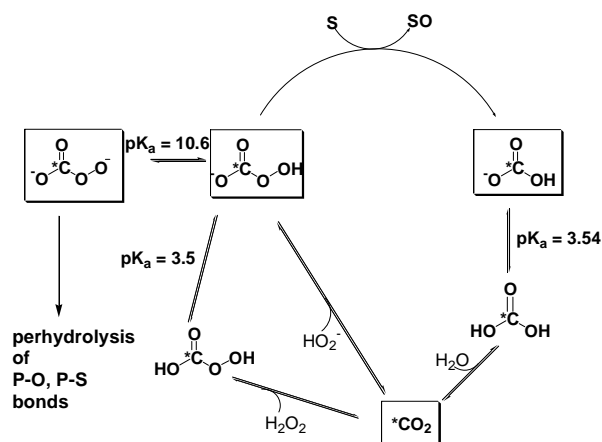
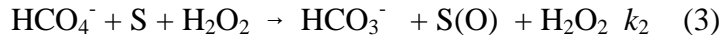
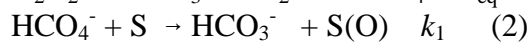
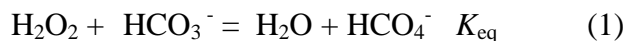
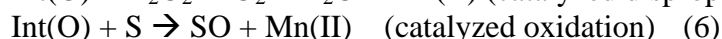
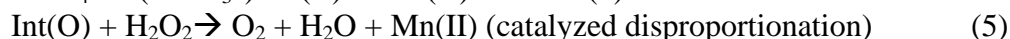
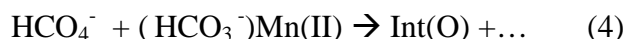


Figure 1. Formation of peroxydicarbonate (HCO_4^-) from bicarbonate (HCO_3^-) and hydrogen peroxide (H_2O_2). Oxidation of a substrate S regenerates the catalyst, and the oxidant peroxydicarbonate is regenerated via perhydration of carbon dioxide. The dianion is a nucleophile and attacks P-O and P-S bonds in V agents along with OOH^- .

The general mechanism for oxidations by BAP is given in eqs 1 - 3.



However, work by Dr. Bennett, Dr. Burke, and Dr. Ramdon described below suggests far more complex mechanisms may operate for certain substrates. The reaction of equation 1 proceeds with the intermediacy of CO_2 as shown in Figure 1. Although it is well understood that metal complexes (e.g., Zn(II)) can accelerate the equilibration of eq 1, a more dramatic effect of metals (especially Mn(II)) is observed in the oxidation reaction of eqs 2 or 3. A working kinetic scheme for such Mn(II) reactions is summarized in eqs 4-6.



The species Int(O) may actually indicate a mixture of reactive intermediates with high-valent Mn and/or radicals. The precise reactivity and degree of competition between paths 5 and 6 will depend on the conditions and the nature of the substrate S.

Note that figures, equations, etc. in the following sections begin in sequence for each individual section.

II. FORMATION OF PEROXYMONOCARBONATE AND THE ROLE OF CO_2

We have devoted significant effort to determine the kinetic constants that control the equilibration of peroxymonocarbonate formation via the CO_2 pathway shown in Figure 1 of section I. This interest was in part driven by curiosity about a remarkable feature of BAP chemistry: the peracid is prepared in near neutral pH solutions. The structure of peroxymonocarbonate, HOOCO_2^- , is analogous to peroxides such as peroxymonosulfate (HOOSO_3^-), peroxyacetic acid ($\text{CH}_3\text{C(O)OOH}$) and peroxyxynitrite (ONOO^-), which, in contrast to HCO_4^- , can only be prepared practically by the reaction of corresponding acids with hydrogen peroxide at low pH in aqueous solutions. Strong acids are commonly used not only to catalyze the reaction but also to provide dehydrating conditions that favor equilibrium formation of peroxyacids. As shown in the figure, we expect that the perhydration of CO_2 by either HOOH or HOO^- will contribute to the overall rate of equilibration. Thus, the rapid formation of the peroxymonocarbonate ion at neutral pH is attributable to the relatively high concentration of the acid anhydride (i.e., CO_2) under those conditions.

To follow the reaction, double pH jump experiments were carried out at low temperature (0°C). First 99% enriched CO_2 was generated in situ by addition of CH_3COOH . Acetic acid was chosen because various organic acid anions were reported to be inactive as catalysts. The ^{13}C NMR spectrum of the resulting solution, mixed with H_2O_2 (1M), has a single peak at 124.54 ppm. Neither $\text{H}_2\text{CO}_3/\text{HCO}_3^-$ nor $\text{H}_2\text{CO}_4/\text{HCO}_4^-$ peaks were detected in the spectrum. These observations indicate the complete conversion of bicarbonate to CO_2 . The equilibrium $\text{CO}_2(\text{aq}) + \text{H}_2\text{O}_2 \rightarrow \text{H}_2\text{CO}_4$ (reaction 8, Table 1 below) is therefore strongly favored to the left at low pH as

for the analogous carbon dioxide hydration equilibrium. The second pH jump was achieved by addition of tribasic sodium phosphate which has low catalytic activity in carbon dioxide hydration. Two new NMR signals at 158.92 and 160.42 ppm, appeared as a result of pH increase and are attributed to the formation of $\text{H}_2\text{CO}_4/\text{HCO}_4^-$ and $\text{H}_2\text{CO}_3/\text{HCO}_3^-$ correspondingly. The NMR spectra show that the relative amount of peroxydicarbonate produced around 400s depends on the pH value. At pH 6.8, roughly equal amounts of HCO_4^- and HCO_3^- are formed, while the increase of pH causes significant growth of HCO_4^- (Figure 1.)

Table 1 shows the complete reaction scheme used to model the equilibration reaction at low temperature.

Table 1 Kinetic equations and their equilibrium and rate constants for the simulation of peroxydicarbonate formation ($T = 0^\circ\text{C}$).

Reaction	Equilibrium constants	Rate constants
1. ^a $\text{CO}_2(\text{g}) = \text{CO}_2(\text{aq})$	$K_1 = 6.20 \times 10^{-1}$	$k_1 = 7.78 \times 10^{-4} \text{ s}^{-1}$ $k_{-1} = 1.25 \times 10^{-3} \text{ s}^{-1}$
2. $\text{HCO}_3^- + \text{H}^+ = \text{H}_2\text{CO}_3$	$K_2 = 2.33 \times 10^3 \text{ M}^{-1}$	$k_2 = 1.40 \times 10^{11} \text{ M}^{-1}\text{s}^{-1}$ $k_{-2} = 6.01 \times 10^7 \text{ s}^{-1}$
3. $\text{H}_2\text{CO}_3 = \text{CO}_2(\text{aq})$	$K_3 = 8.01 \times 10^2$	$k_3 = 3.74 \text{ s}^{-1}$ $k_{-3} = 4.67 \times 10^{-3} \text{ s}^{-1}$
4. $\text{HCO}_3^- = \text{CO}_2(\text{aq}) + \text{HO}^-$	$K_4 = 2.00 \times 10^{-9} \text{ M}$	$k_4 = 4.42 \times 10^{-6} \text{ s}^{-1}$ $k_{-4} = 2.07 \times 10^3 \text{ M}^{-1}\text{s}^{-1}$
5. ^b $\text{CO}_2(\text{aq}) + \text{H}_2\text{O}_2 = \text{H}_2\text{CO}_4$	$K_5 = 4.12 \times 10^{-4} \text{ M}^{-1}$	$k_5 \geq 1.55 \times 10^{-2} \text{ M}^{-1}\text{s}^{-1}$ $k_{-5} \geq 3.76 \times 10^1 \text{ s}^{-1}$
6. $\text{H}_2\text{CO}_4 = \text{HCO}_4^- + \text{H}^+$	$K_6 = 4.29 \times 10^{-4} \text{ M}$	$k_6 = 6.01 \times 10^7 \text{ s}^{-1}$ $k_{-6} = 1.40 \times 10^{11} \text{ M}^{-1}\text{s}^{-1}$
7. ^b $\text{H}_2\text{O}_2 = \text{HOO}^- + \text{H}^+$	$K_7 = 7.01 \times 10^{-13} \text{ M}$	$k_7 = 9.81 \times 10^{-2} \text{ E-02 s}^{-1}$ $k_{-7} = 1.40 \times 10^{11} \text{ M}^{-1}\text{s}^{-1}$
8. ^b $\text{CO}_2(\text{aq}) + \text{HOO}^- = \text{HCO}_4^-$	$K_8 = 2.52 \times 10^5 \text{ M}^{-1}$	$k_8 \geq 1.08 \times 10^3 \text{ M}^{-1}\text{s}^{-1}$ $k_{-8} \geq 4.29 \times 10^{-3} \text{ s}^{-1}$
9. ^c $\text{HCO}_3^- + \text{ZnL}(\text{H}_2\text{O})^{2+} = \text{CO}_2 + \text{ZnL}(\text{OH})^+$	$K_9 = 1.70 \times 10^{-2}$	$k_{cat}^d = 5.60 \times 10^1 \text{ M}^{-1}\text{s}^{-1}$ $k_{cat}^h = 3.30 \times 10^3 \text{ M}^{-1}\text{s}^{-1}$

^a the equilibrium was removed from mechanism and $[\text{CO}_2]_0$ was changed to ideal concentration (0.073M) at 0°C after the best fit was found

^b perhydration (5) and hydroperoxide addition reactions (7, 8) were removed from mechanism, one at a time for clarification of their contribution

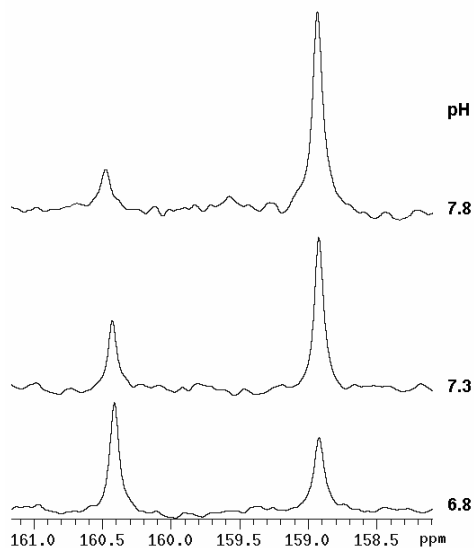


Figure 1

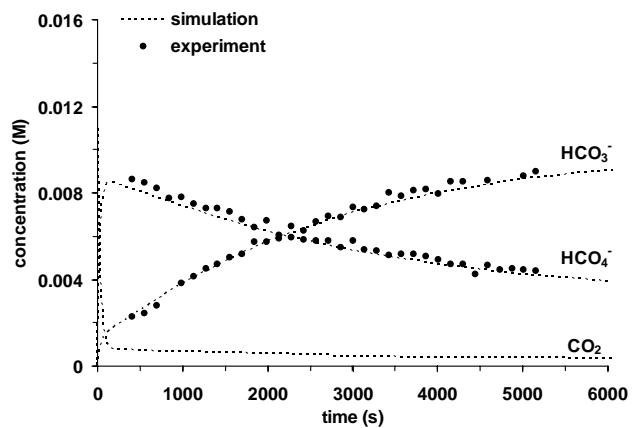
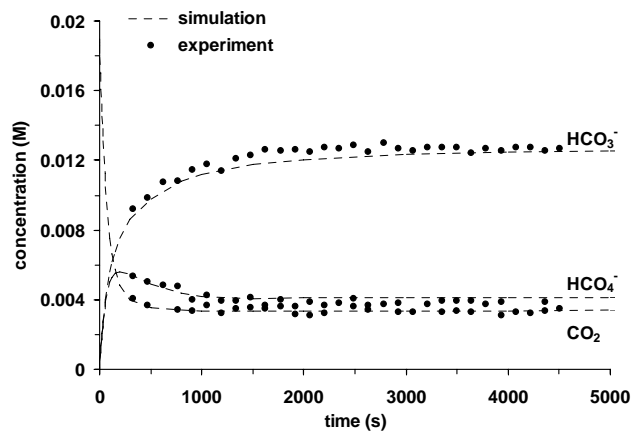


Figure 2 Example of simulated and observed data (best fit) for CO_2 hydration and perhydration reactions at pH 6.8 (top) and 7.8 (bottom). The mechanism includes reaction 8; reaction 5 is not used in this set of fits.

Kinetic simulations of double pH jump experiments demonstrate that the mechanism of bicarbonate (HCO_3^-) reaction with hydrogen peroxide involves the formation of CO_2 as an intermediate and reaction of CO_2 with H_2O_2 and its conjugate base HOO^- . The lower limits for rate constants of CO_2 reaction with H_2O_2 ($1.55 \times 10^{-2} \text{ M}^{-1}\text{s}^{-1}$) and HOO^- ($1.08 \times 10^3 \text{ M}^{-1}\text{s}^{-1}$) to form peroxymonocarbonate (HCO_4^-) were estimated by numerical simulations. Unfortunately, even at the lowest temperature used (0°C) the NMR data points (for reaction times $< 200 \text{ s}$) needed to establish the absolute values of the two rate constants cannot be obtained. The hydroperoxide (HOO^-) and hydroxide addition pathways are likely to be competitive, and the contribution of HOO^- to initial HCO_4^- formation increases with increasing pH.

Formation of peroxymonocarbonate by the reaction of HCO_3^- with H_2O_2 can be significantly accelerated by carbonic anhydrase and $[\text{Zn(II)L(H}_2\text{O)}]^{2+}$ ($\text{L} = 1,4,7,10\text{-tetraazacyclododecane}$), a model complex for the enzyme. The facile nature of the $\text{CO}_2/\text{HCO}_3^-$ equilibrium allows for rapid formation of the peroxymonocarbonate ion at physiological pH values. This catalysis has been added to the model successfully. (These results suggest that carbonic anhydrase can play a central role in the formation of the reactive oxygen species HCO_4^- in vivo – see section IX.)

III. ROLE OF TRACE METALS IN STABILITY OF BAP SOLUTIONS

The stability of BAP solutions toward disproportionation is an important characteristic for practical uses in CWA/BWA decon applications. We wondered what the role of trace contaminant metals such as Mn(II) could play in the stability of the solutions, and decided to determine the rate law for such catalyzed disproportionations. In related work described in a later section of this report, we continued our long term investigations of BAP solution stabilities. The available literature proposes a free radical pathway based on Fe(II) chemistry, which is supported by work done by Sychev in the late 1970's using the hydroxyl radical trap *N,N*-dimethyl-4-nitrosoaniline.

The role of Mn(II) in the disproportionation of hydrogen peroxide in bicarbonate solutions has been examined by Dr. Burke and Dr. Ramdon. The hydrogen peroxide concentration was held constant at 0.30 M, sodium bicarbonate concentration ranged from 0.00 – 0.60 M, Mn(II) concentration ranged from 0.0 – 30.0 μM , and the ionic strength was held constant at 1.00 M using sodium acetate. The observed rate constants for the catalyzed disproportionation reaction were as much as 20 times faster than the background disproportionation with no metal present. Plots of k_{obs} vs $[\text{H}_2\text{O}_2]$ gave linear first order fits. The dependence on Mn(II) has been determined to be first order for the range 0.0 – 7.0 μM , as seen in Figure 1. The first order dependence in this range indicates only 1 metal center is found in the transition state of the reaction. This is significant since much of the current literature on metal catalyzed hydrogen peroxide disproportionation focuses on multiple metal center complexes.

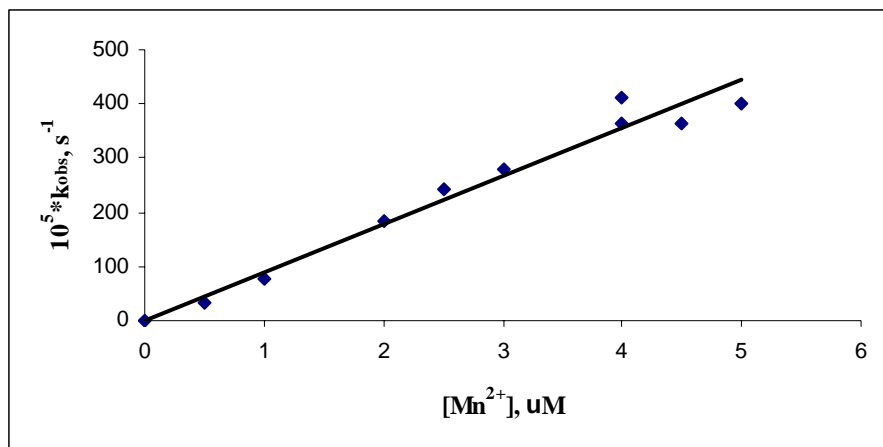


Figure 1

The dependence on bicarbonate has been determined to be second order for the range of 0.00 – 0.60 M, using a constant Mn(II) concentration of 4.0 μM , as seen in Figure 2. This reveals that two bicarbonate ions are present in the transition state. Presumably, one of these bicarbonate ions exists as the peroxy carbonate ion, while the other is simply coordinated to the metal ion. The rate law at pH = 8.5 is therefore

$$R = k_{\text{cat}} [\text{HCO}_3^-]^2 [\text{Mn}] [\text{H}_2\text{O}_2]$$

The value of $k_{\text{cat}} = 5700 \text{ M}^{-2}\text{s}^{-1}$ at 298 K in water.

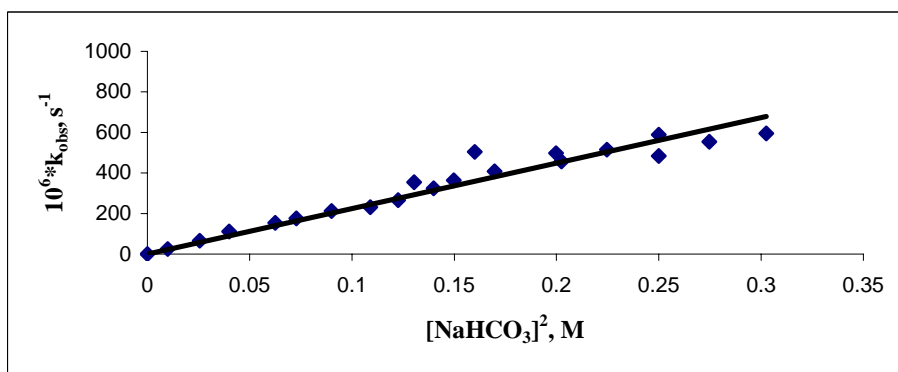
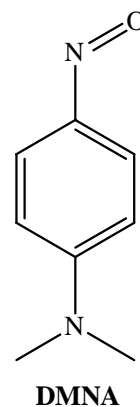


Figure 2

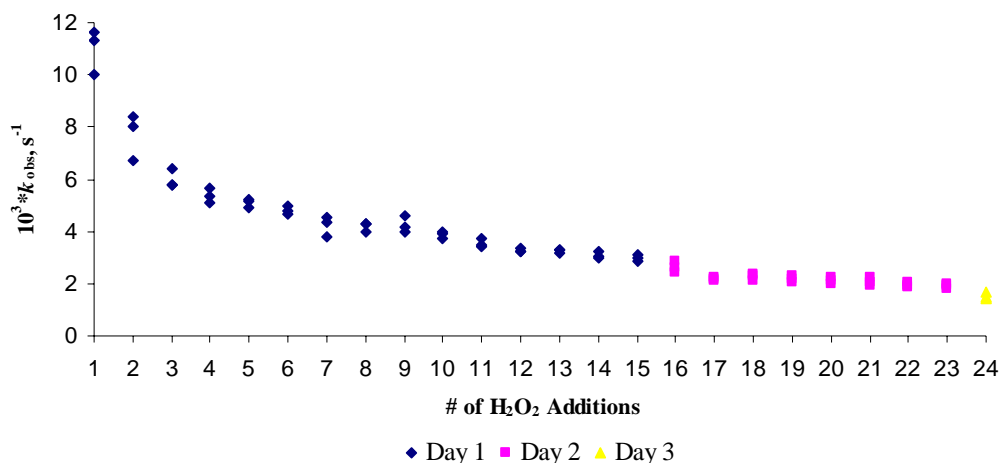
In the late 1970's, Sychev proposed that the disproportionation of hydrogen peroxide by Mn(II) in bicarbonate ions proceeded via a free hydroxyl radical pathway. This conclusion was reached by experiments performed using the hydroxyl radical trap *N,N*-dimethyl-4-nitrosoaniline (DMNA), shown at right. Sychev noted that with increasing amounts of the radical trap added, the production of O_2 (g) from the disproportionation decreased. This led Sychev to conclude the reaction proceeded through a free hydroxyl radical mechanism. Reactions using the radical trap DMNA have been conducted using the Mn(II) / H_2O_2 / bicarbonate system. The isolated organic products appear to be the result of *N*-dealkylation and include *N*-methyl-4-nitroaniline and 4-nitroaniline. The



isolation of these products indicates a different pathway may be present than that proposed by Sychev. Miwa et al have extensively studied the *N*-dealkylation reaction of cytochrome P-450. These metal dependent *N*-dealkylating systems are believed to have a high valent metal-oxo species in the transition state. In view of KIE values close to unity, it is believed that breaking the α -carbon hydrogen bond is not rate determining. Based on this information, a single electron transfer mechanism is proposed to explain the KIE data. From these finding, we believe the mechanism proposed by Sychev may be incomplete.

The reactive Mn complex is thought to have a high valence metal center that can react via direct oxygen transfer or radical mechanisms. Our later work is centered on characterizing the complex and understanding the reaction mechanism. Such studies are important in considering the storage and formulation of BAP decon solutions and suggest methods for inhibiting peroxide decomposition. In addition, we believe that Mn/BAP may have broader applications for environmental and chemical/biological decontamination. In general, the data support the formation of a reactive intermediate, perhaps a Mn(IV)-oxo complex that can transfer O in heterolytic reactions or decompose to release radicals in the disproportionation of peroxide for oxidation of other substrates.

The catalytic lifetime for the manganese-catalyzed hydrogen peroxide disproportionation is an important characteristic for practical application in CWA/BWA decon applications. We were curious about the catalytic lifetime of the spent manganese/bicarbonate solutions after peroxide disproportionations were completed. Hydrogen peroxide solutions were allowed to decompose until the peroxide was no longer detected spectrophotometrically. The peroxide concentration was then recharged to near the original concentration at which time the disproportionation rate was monitored spectrophotometrically. A graph of k_{obs} vs. number of times the solution was recharged is shown in Graph 1.



Graph 1 - k_{obs} vs. cycle number

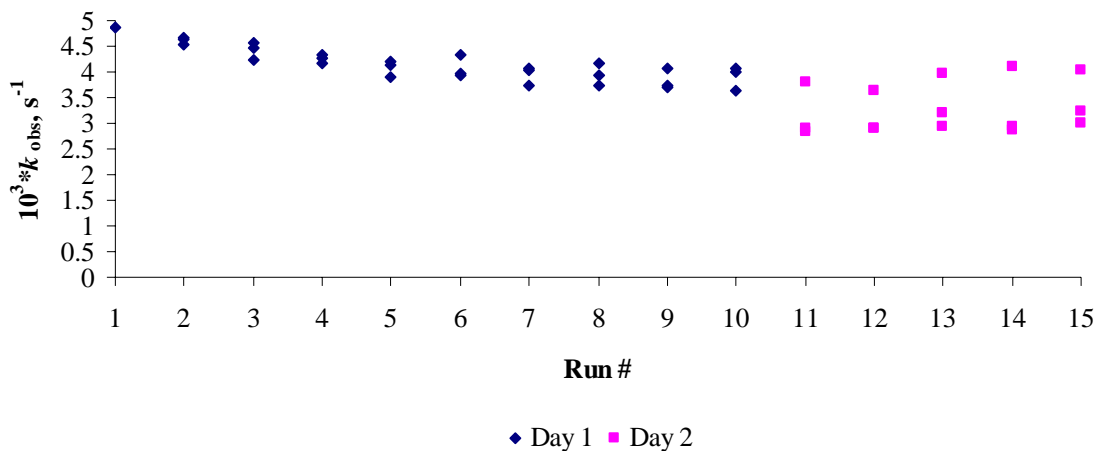
During these experiments, two 16 hour delays were included to show that the catalyst can be regenerated even after relatively long periods of inactivation when no peroxide is present. These two delays are between runs 15 and 16 and runs 23 and 24. From this data it should be noted that the k_{obs} drops by about 90% over the 24 runs. We then wanted to understand why this loss of activity was seen for these solutions.

A number of factors could be responsible for the loss of activity seen in Graph 1. Two of the factors believed to be most significant include loss of bicarbonate during the cycled reactions and precipitation of the metal catalyst.

During the course of peroxide disproportionation, oxygen gas evolution is vigorous enough to lead to concerns that the bicarbonate concentration may not be stable during the reactions. As oxygen is evolved, carbon dioxide may be displaced from the reaction solutions causing the bicarbonate concentration to fall during the disproportionation reactions. To examine this issue, a large-scale reaction was allowed to cycle 10 times under the same conditions used for the spectrophotometric investigation. The spent solution was then analyzed for the change in bicarbonate concentration. It was found that during these 10 cycles, nearly $\frac{1}{2}$ of the bicarbonate concentration was lost. Since the kinetic examination has revealed a second order dependence on the bicarbonate concentration, this loss of bicarbonate results in a 75% loss of reactivity.

The second factor examined to explain the loss of catalytic activity seen for the manganese/bicarbonate solutions is the precipitation of the metal catalyst. Commercial hydrogen peroxide solutions are stabilized using phosphoric acids. As the hydrogen peroxide is being recharged after each cycle, more phosphates are being added to the cycled solutions. This may be causing metal phosphate salts to precipitate. An examination of the commercial hydrogen peroxide solutions by malachite green assay revealed that our stock contains ~ 4 mM phosphate. For each catalytic cycle, ~ 25 μ M phosphate is added to the solution.

A second cycle study was performed to examine what the effect on the catalytic lifetime of the manganese/bicarbonate solutions. Sodium bicarbonate is added during each cycle to help maintain the bicarbonate concentration. Also, the hydrogen peroxide was distilled to remove the phosphate stabilizer. The graph of k_{obs} vs. cycle number is shown in Graph 2. The k_{obs} in Graph 2 show much less decay than those of Graph 1.



Graph 2 - k_{obs} vs. cycle number

The loss of activity seen between run 1 and run 15 is about 30% while the loss for the first catalyst lifetime study showed an 80% loss between the same runs. This residual loss of activity is likely due to both dilution effects and the inability to fully control the bicarbonate concentration.

IV. INHIBITION OF BAP DISPROPORTIONATION BY COORDINATING ANIONS AND EFFECT OF SOLVENT COMPOSITION

It is well known that addition of chelating ligands, such as EDTA, will significantly reduce metal-catalyzed decomposition of peroxides. This has practical importance for decon applications because decomposition of peroxide is a major hurdle to widespread use of peroxide in formulations. We wondered if the inhibition of Mn catalyzed decomposition could be explained purely by metal binding, so Dr. Ramdon investigated a series of ligands with known binding constants for Mn(II). In addition, he investigated the impact of co-solvents on the decomposition rate. The inhibition studies also complemented our other kinetic studies on Mn/BAP chemistry.

The carboxylate anions acetate, succinate and oxalate are structurally similar to bicarbonate with binding constants to Mn(II) of 6.3,⁽¹⁾ 30,⁽²⁾ and 1584⁽¹⁾ respectively. The effect of these on the decomposition of H₂O₂ by the Mn²⁺ / HCO₃⁻ pair was studied to determine the environment of the metal during the reaction. Manganese ion, independent of its oxidation state, and the HCO₃⁻ ion are both necessary to effect the disproportionation of H₂O₂. To date, a literature search has shown that no other simple ligand displays this unique behavior regardless of its similarity to the carbonate. There seems to be a significant difference between bicarbonate and carboxylate which accounts for this behavior.

The combination of Mn(II) / HCO₃⁻ / H₂O₂ is a very efficient oxidant for the epoxidation of selected alkenes. The mechanism for this action appears to be radical driven, unlike the oxidation of sulfides by HCO₃⁻ / H₂O₂ without Mn(II). Some weakly soluble organic substrates require the use of co-solvent mixtures as the reaction medium. The effect that such solvents have on the background disproportionation of H₂O₂ should be understood. This issue was also addressed.

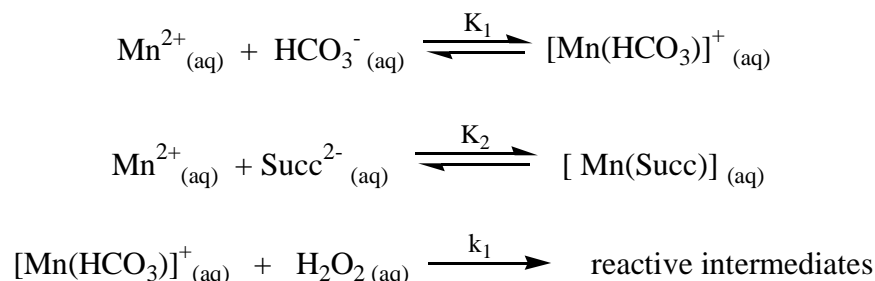
Experimental

Effect of complexing ligands: The disproportionation of H₂O₂ was monitored using UV-VIS Spectrophotometry under the following conditions: [H₂O₂]₀ = 0.10 M, [HCO₃⁻]₀ = 0.10 M, [Mn²⁺]₀ = 3.0 μM, I = 0.40 M, λ = 280 nm, and T = 25.0 °C. Appropriate amounts of H₂O, H₂O₂, HCO₃⁻, ligand and supporting electrolyte were pipetted into 1 cm quartz cuvettes and allowed to equilibrate in the thermostated multi-cell transport of the HP8453 Spectrophotometer. These were then spiked with Mn(II) solution, mixed and the absorbance monitored using the ChemStation Software with pure H₂O as reference. All reactions, except the very slow, were monitored for at least three half-lives. Absorbance vs time traces fitted first-order decay equations for at least two half-lives with acceptable errors. Pseudo first-order rate constants (k_{obs}) were independent of wavelength over range 260 > λ > 290 nm.

Effect of organic solvents: The decomposition of H₂O₂ by Mn²⁺ / HCO₃⁻ was studied in water-organic co-solvent mixtures. The solvents used were ethanol, *t*-butanol and acetonitrile. A similar approach as described above was used with the appropriate blanks.

Results and Discussion

Effect of Complexing ligands: Tables 1-3 show that the addition of ligands to the $\text{Mn}^{2+} / \text{HCO}_3^- / \text{H}_2\text{O}_2$ mixture decrease the pseudo first order rate constant for the decomposition of H_2O_2 . This seems to be directly related to concentration of the ligand and its binding constant to Mn^{2+} relative to HCO_3^- . We assume that the relevant pre-equilibria and simplest form of an elementary step can be represented by Scheme 1 using succinate dianion as the suppressing ligand.



Scheme 1. Relevant pre-equilibrium reactions in the suppression of the rate of decomposition of hydrogen peroxide by complexing ligands

Table 1. The effect of the concentration of acetate anion on the pseudo first-order rate constant for decomposition of H_2O_2 by $\text{Mn}^{2+} / \text{HCO}_3^-$. $T = 25.0\text{ }^\circ\text{C}$, $[\text{H}_2\text{O}_2]_0 = 0.10$ & 0.20 M , $[\text{HCO}_3^-]_0 = 0.10\text{ M}$, $I = 0.40\text{ M}$, $\lambda = 280\text{ nm}$, $\text{pH} = 8.46$, $[\text{Mn}^{2+}]_0 = 3.0\text{ }\mu\text{M}$.

[Acetate] ₀ / mM	$k_{\text{obs}} / 10^{-4}\text{ s}^{-1}$	
	$[\text{H}_2\text{O}_2]_0 = 0.10\text{ M}$	$[\text{H}_2\text{O}_2]_0 = 0.20\text{ M}$
0	3.60 ± 0.09	2.69 ± 0.08
50	3.45 ± 0.09	2.63 ± 0.08
100	3.37 ± 0.08	---
150	3.21 ± 0.08	2.45 ± 0.07
200	3.12 ± 0.08	2.35 ± 0.07
250	2.95 ± 0.07	2.25 ± 0.07

Table 2. The effect of the concentration of succinate anion on the pseudo first-order rate constant for decomposition of H_2O_2 by $\text{Mn}^{2+} / \text{HCO}_3^-$. $T = 25.0\text{ }^\circ\text{C}$, $[\text{H}_2\text{O}_2]_0 = 0.10\text{ M}$, $[\text{HCO}_3^-]_0 = 0.10\text{ M}$, $I = 0.40\text{ M}$ (NaClO_4), $\lambda = 280\text{ nm}$, $\text{pH} = 8.34$, $[\text{Mn}^{2+}]_0 = 3.0\text{ }\mu\text{M}$.

[Succinate] ₀ / mM	$k_{\text{obs}} / 10^{-4}\text{ s}^{-1}$
0.0	3.69 ± 0.07
20	3.27 ± 0.05
40	3.00 ± 0.04
60	2.64 ± 0.02
80	2.37 ± 0.02
100	2.12 ± 0.02

Table 3. The effect of the concentration of oxalate anion on the pseudo first-order rate constant for decomposition of H_2O_2 by $\text{Mn}^{2+} / \text{HCO}_3^-$. $T = 25.0\text{ }^\circ\text{C}$, $[\text{H}_2\text{O}_2]_o = 0.10\text{ M}$, $[\text{HCO}_3^-]_o = 0.10\text{ M}$, $I = 0.40\text{ M}$ (KCl), $\lambda = 280\text{ nm}$, $\text{pH} = 8.40$, $[\text{Mn}^{2+}]_o = 3.0\text{ }\mu\text{M}$.

[Oxalate] _o / mM	$k_{\text{obs}} / 10^{-4}\text{ s}^{-1}$
0.0	3.79 ± 0.07
20	1.22 ± 0.02
40	0.61 ± 0.02
60	0.36 ± 0.03
80	0.23 ± 0.09
100	0.20 ± 0.07

The equilibrium concentration of manganese(II) bicarbonate, $[\text{Mn}(\text{HCO}_3)]^+$ can be derived, Eqn 1.

$$[\text{Mn}(\text{HCO}_3)]^+ = \frac{K_1[\text{HCO}_3]_T[\text{Mn}]_T}{1 + K_1[\text{HCO}_3]_T + K_2[\text{Succ}]_T} \quad (1)$$

If this is the only complex that reacts with H_2O_2 , then the pseudo first order rate constant, k_{obs} , for the decomposition of hydrogen peroxide can be written as Eqn 2.

$$k_{\text{obs}} = \frac{k_1 K_1[\text{HCO}_3]_T[\text{Mn}]_T}{1 + K_1[\text{HCO}_3]_T + K_2[\text{Succ}]_T} \quad (2)$$

This can be rearranged to the linear form shown in Eqn 3.

$$\frac{K_1[\text{HCO}_3]_T[\text{Mn}]_T}{k_{\text{obs}}} = \frac{1 + K_1[\text{HCO}_3]_T}{k_1} + \frac{K_2}{k_1}[\text{Succ}]_T \quad (3)$$

Using a literature value of $K_1 = 18.6\text{ M}^{-1}$,⁽³⁾ this latter equation can be fitted to data from Table 2 which gives a straight line with intercept of $(1.47 \pm 0.03) \times 10^{-2}\text{ M s}$ and a slope of $(1.11 \pm 0.05) \times 10\text{ s}$ - Figure 1. The parameters k_1 and K_2 were calculated as $194 \pm 7\text{ M}^{-1}\text{ s}^{-1}$ and $22 \pm 1\text{ M}^{-1}$ respectively, under these conditions. This value of K_2 is comparable to previous reports of 181 M^{-1} at $I = 0.0\text{ M}$ ⁽¹⁾ and 30 M^{-1} at $I = 0.20\text{ M}$ ⁽²⁾ both with $T = 25.0\text{ }^\circ\text{C}$. Our experiments were conducted at a higher ionic strength, $I = 0.40\text{ M}$, and hence K_2 was predicted to be less than 30, in agreement with the calculation.

Similar manipulation of data in tables 1 and 3 also yield straight lines as summarized in Table 4 ($k_1 = 140 \pm 1\text{ M}^{-1}\text{ s}^{-1}$ when $[\text{H}_2\text{O}_2]_o = 0.20\text{ M}$). The extent of decrease in the pseudo first order rate constant is directly related to the binding of Manganese(II) by the non-bicarbonate ligands. Of the ligands studied, oxalate has the largest binding constant for Manganese(II), 1584 M^{-1} at $I = 0.10\text{ M}$,⁽¹⁾ and is comparatively the most effective at suppressing the decomposition of hydrogen peroxide - Table 3. It should be noted that if these ligands were precipitating dissolved Manganese(II) a similar decrease in pseudo first order rate constant would be observed with increase in ligand concentration. However the experimental concentrations are below saturation

amounts ($[Mn^{2+}][C_2O_4^{2-}] < K_{sp} = 4.6 \times 10^{-6} M^2$).⁽⁴⁾ It can be concluded that the effect observed is due to complexation of Manganese(II) decreasing the equilibrium concentration of Manganese(II) bicarbonate. Other experiments have been done to show that the addition of millimolar quantities of DTPA (diethylenetriaminepentaacetic acid) quench the reaction immediately.

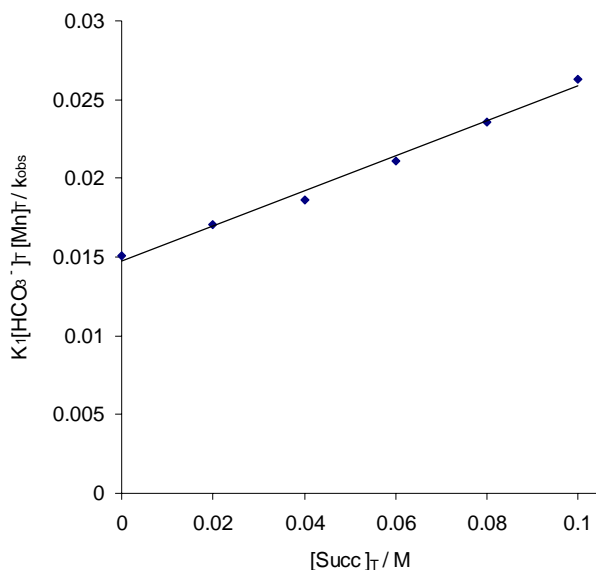


Figure 1. Plot of $K_1[HCO_3^-]_T[Mn]_T / k_{obs}$ Vs $[Succ]_T$ for the decomposition of H_2O_2 with Mn^{2+}/HCO_3^- in aqueous solution. $[H_2O_2]_o = 0.10 M$, $[HCO_3^-]_o = 0.10 M$, pH = 8.34, $[Mn^{2+}]_o = 3.0 \mu M$, $I = 0.40 M$ (NaClO₄), $T = 25.0 \text{ }^\circ C$, $\lambda = 280 \text{ nm}$.

Table 4. Calculated equilibrium constants for the complexation of aqueous Mn^{2+} by carboxylate ligands. $T = 25.0 \text{ }^\circ C$, $[H_2O_2]_o = 0.10 M$, $[HCO_3^-]_o = 0.10 M$, $I = 0.40 M$ (KCl), $\lambda = 280 \text{ nm}$, pH = 8.40, $[Mn^{2+}]_o = 3.0 \mu M$.

Ligand	$K_{2,lit}$ at 25 °C / M^{-1}	K_2 / k_1	<i>Expt</i> K_2 / M^{-1} I = 0.40 M
Acetate	6.3 (I = 0.1 M)	0.0132	2.6 ± 0.2 2.3 ± 0.1 *
Succinate	30 (I = 0.2 M)	0.111	22 ± 1
Oxalate	1584(I = 0.1M)	2.82	550 ± 40
Phosphate	NA	≈ 2.5	

* $[H_2O_2]_o = 0.20 M$

These results highlight the unique behavior of the Mn^{2+}/HCO_3^- pair towards the disproportionation of hydrogen peroxide in aqueous solution. The effect of such carboxylate

ligands were explored primarily because dimers of Manganese have been prepared with carboxylate ligands acting as bridges.⁽⁵⁾ Such dimers, of various oxidation states, are capable of rapid decomposition of H₂O₂.^(6,7) It was assumed that if such dimers are formed in the presence of HCO₃⁻ the action of carboxylate would catalyze decomposition and not retard rates. Some manganese dimers were prepared,^(5,8) but these readily decomposed in aqueous solution. Spectral characterization was possible in acetonitrile/water mixture which disappeared rapidly with H₂O₂ addition. Their ability to decompose excess H₂O₂ continued after spectral disappearance the Mn dimer. This could mean that the dimer is intact and spectrally featureless (characteristic of Mn²⁺ ions) or the degradation products are capable of accomplishing the reaction. EPR studies have shown that Mn²⁺_{aq} signal disappears when in H₂O₂/HCO₃⁻. One possible interpretation is that a Mn²⁺ dimer is dominant in solution or some other EPR silent Mn species. The kinetics of decomposition of H₂O₂ by such dimers was too fast for the HP8453 and they have large absorbance in the wavelength range of interest.

Effect of organic solvents: The reaction of H₂O₂/HCO₃⁻/Mn²⁺ could not be studied in acetonitrile-water due to significant absorbance from reaction products. This same reaction showed zero order profile in t-butanol with the formation of spectrally interfering species toward the end of the reaction. Results could only be generated in ethanol / water mixtures.

Ethanol increases the rate constant, k_{obs}, for decomposition of H₂O₂ up to 45 % (v/v) as shown in Figure 2. Beyond that point, under these conditions, there is a recorded decrease in the rate constant. This appears to be due to the lower solubility of the active HCO₃⁻ salt at higher compositions of ethanol. It should be noted however that provided the saturation point has not been achieved, ethanol increases the rate of the reaction. That point is further re-enforced in Figure 3, which shows that the maximum k_{obs} is obtained at a higher [HCO₃⁻]₀ when ethanol content is smaller. The assumption that the salt being precipitated is Mn(HCO₃)₂, could easily be made, but that was not confirmed with Figure 4. If K_{sp} of Mn(HCO₃)₂ was being exceeded then both the dependence on [Mn²⁺] and [HCO₃⁻] would pass through a maximum. Since only [HCO₃⁻] shows this maximum, the effect of precipitation is more sensitive to [HCO₃⁻] than [Mn²⁺]. An understanding of the results can be made when the definition of K_{sp} = [Mn²⁺][HCO₃⁻]² is considered. Since the ionic product is related to the square of [HCO₃⁻] then K_{sp} is more rapidly exceeded when [HCO₃⁻] is varied compared to [Mn²⁺].

The results of Figure 3 are further compounded by the fact that the common ion effect from K⁺ in the electrolyte plays a role. The [K⁺] in these experiments is fixed at 0.30 M being derived from both KHCO₃ and KCl. If this limited the [HCO₃⁻] then there should be a sharp break point, not a curved maximum. The precipitation of KHCO₃ could co-precipitate Mn²⁺ accounting for the observed decrease at higher [HCO₃⁻]. Carbonate salts can be removed from 80 % sodium chlorite by recrystallization in ethanol-water, producing 99 % chlorite – carbonates clearly have poor solubility in ethanol.

The common ion effect is not a factor in Figure 4. It would be interesting to see the result if these experiments were repeated with an electrolyte at higher ionic strength. The result does confirm some mixed order dependence (> first order) on [Mn²⁺] in ethanol water different from pure aqueous media, suggesting that dimers or other polynuclear aggregates may have increasing kinetic importance in those conditions.

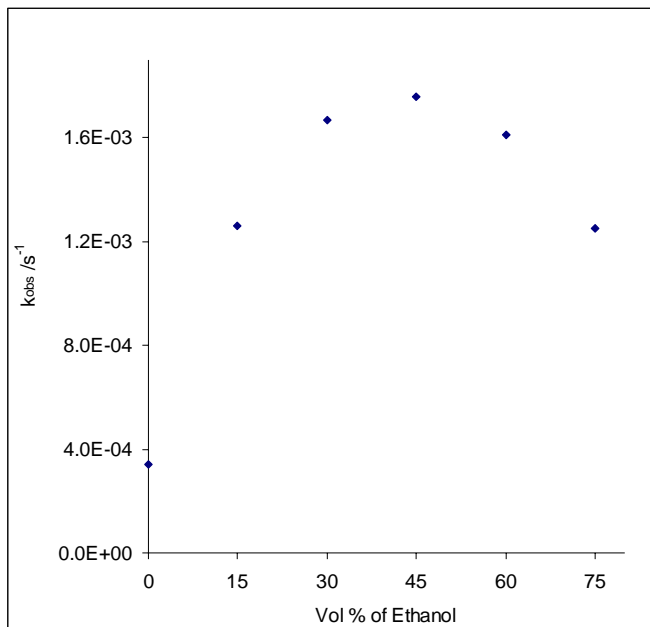


Figure 2. The effect of solvent composition on the Mn^{2+} catalyzed decomposition of H_2O_2 . $T = 25.0\text{ }^\circ C$, $[HCO_3^-]_0 = 0.10\text{ M}$, $[H_2O_2]_0 = 0.10\text{ M}$, $[Mn^{2+}]_0 = 5.0\text{ }\mu M$, $I = 0.10\text{ M}$.

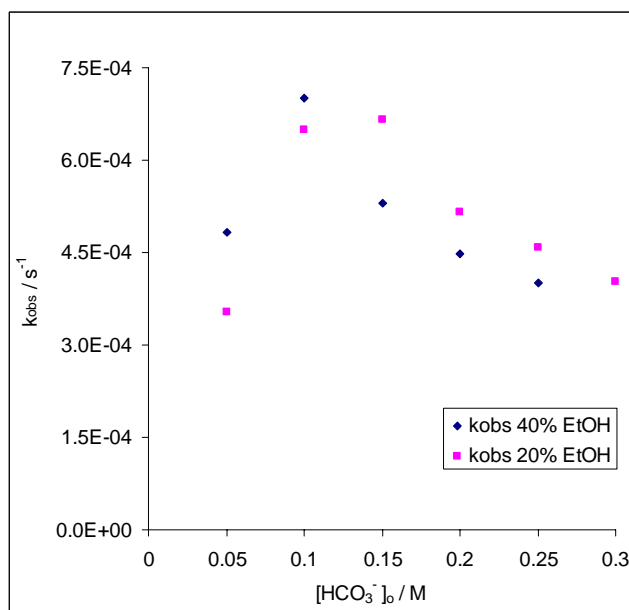


Figure 3. Effect of $[HCO_3^-]$ on the Mn^{2+} catalyzed decomposition of H_2O_2 in water-ethanol solution. $T = 25.0\text{ }^\circ C$, $I = 0.30\text{ M}$ (KCl), $[H_2O_2]_0 = 0.10\text{ M}$, $\lambda = 270\text{ nm}$, $[Mn^{2+}] = 3.0\text{ }\mu M$.

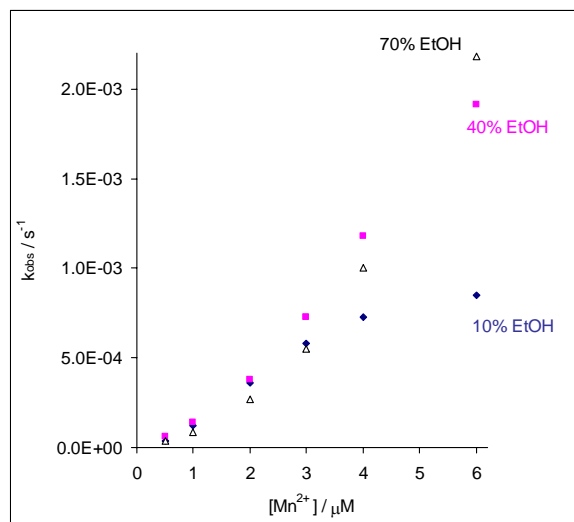


Figure 4. Effect of $[\text{Mn}^{2+}]$ on the catalytic decomposition of H_2O_2 . $[\text{H}_2\text{O}_2]_0 = 0.10 \text{ M}$, $[\text{HCO}_3^-]_0 = 0.10 \text{ M}$, $T = 25.0 \text{ }^\circ\text{C}$, $I = 0.10 \text{ M}$.

References (section IV)

- 1) Editors. Martell, A. E.; Smith, R. M., *Critical Stability Constants, Vol 3: Other Organic Ligands*, Plenum Press, London, **1977**, Plenum Press, New York, 5.
- 2) McAuley, A.; Nancollas, G. H., *J. Chem. Soc.*, **1961**, 4458-4463.
- 3) Lesht, D.; Bauman, J., *Inorg. Chem.*, **1978**, 17(12), 3332-3334.
- 4) Chambelain, N.; Hume, J.; Topley, B., *J. Chem. Soc.* **1926**, 2620-2623.
- 5) Dave, B. C.; Czernuszewicz, R. S.; Bond, M. R.; Carrano, C. J., *Inorg. Chem.*, **1993**, 32, 3593-3594.
- 6) Wu, A. J.; Penner-Hahn, J. E.; Pecoraro, V. L., *Chem. Rev.*, **2004**, 104, 903-938.
- 7) Dismukes, G. C. *Chem. Rev.* **1996**, 96, 2909-2926.
- 8) Manchandra, R.; Brudvig, G. W.; de Gala, S.; Crabtree, R. H., *Inorg. Chem.*, **1994**, 33, 5157-5160.

V. LIFETIMES OF INHIBITED BAP SOLUTIONS

Decomposition of bicarbonate-hydrogen peroxide solutions is a concern with their use as a rapid universal “green” decontaminant. We have studied the loss of hydrogen peroxide equivalents versus time to determine long-term storage potentials for peroxy carbonate solutions (Table 1).

Our previous studies have confirmed that hydrogen peroxide in water is stable with a half-life of up to several years (with commercial inhibitors present as received). Results showed added bicarbonate increase hydrogen peroxide decomposition rates, observed with half-lives on the order of several days under most conditions. Various experiments have shown a higher concentration of trace metals present in the sodium salts of both phosphate and bicarbonate. Current projects have also shown that metal-assisted decomposition of hydrogen peroxide is significant when bicarbonate salts are present (see above).

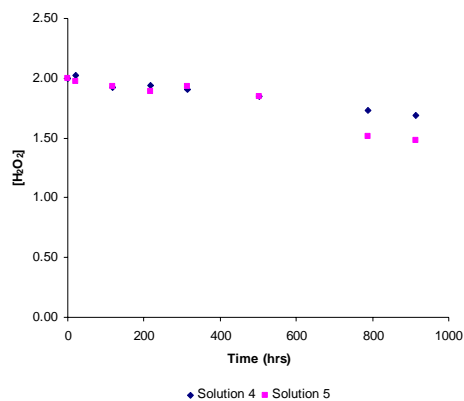
In this particular study a chelating agent, diethylenetriaminepentaacetic acid (DTPA), was used to limit any metal-assisted decomposition, which was hypothesized as a probable cause of peroxide disproportionation due to trace metal contaminants in salt components. The results showed that increasing concentrations of DTPA from 10 μM to 100 μM had no significant effect on decomposition rate (Graph 1) in bicarbonate-free solutions, although it was observed that the DTPA did decrease the rate of decomposition compared to chelate-free solutions (Graph 2). The results indicate that a very low trace metal contaminant is present in the phosphate salts and a minimum amount of DTPA is necessary to limit slow metal-based decomposition. Phosphate salts are considered inert inorganic salts and showed no reactivity with hydrogen peroxide in our previous work. Addition of bicarbonate salts to the solutions dramatically decreased the half-life of decomposition from months to days (Graph 3). DTPA concentrations were increased from 10 μM to 1000 μM and no change in the rate of decomposition was seen (Graph 4). Increases in the decomposition can therefore be attributed to reaction of the peroxy carbonate with hydrogen peroxide. For all reactions no change in pH greater than a half unit was observed, but it is not unusual to observe shifts in pH with time in many (presumably as a result of CO_2 evolution). In general however, trace metal-based decomposition of peroxide is evidently negligible compared to the intrinsic instability of BAP solutions, at least with the components used in this work. Stability could be probably be enhanced for solutions that have unusually high trace metal content (due to metal storage containers, for example) by use of chelate inhibitors, as there is no doubt that Mn and other metals accelerate peroxide decomposition at higher than trace levels we investigated here.

A second part of the study involved using a split solvent system to determine if any change in the decomposition rate was observed. Reactions using CTACl, with and without DTPA, showed a slight decrease in decomposition of hydrogen peroxide versus only water (Graph 5). Ethanol/water (1:4 v/v) solutions showed a slight decrease in the rate of decomposition. A mixture of propylene carbonate/ water (1:1 v/v) showed an even greater decrease in the rate of decomposition compared to ethanol/water solution, CTACl, and pure water (Graph 6). One difference to note is that with the propylene carbonate mixture the pH was 7.6 compared to the other solutions, which had a pH value of ~ 8.6 .

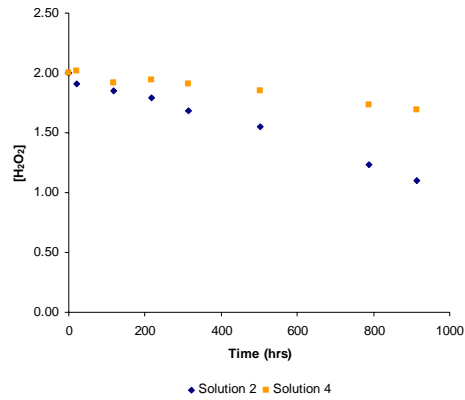
In conclusion, bicarbonate with hydrogen peroxide will form peroxy carbonate, which can react with the remaining hydrogen peroxide to increase the rate of peroxide decomposition. Mixed solvent systems decrease the rate of decomposition allowing for longer storage periods.

Table 1. Solution mixtures, half -lives and relevant data.

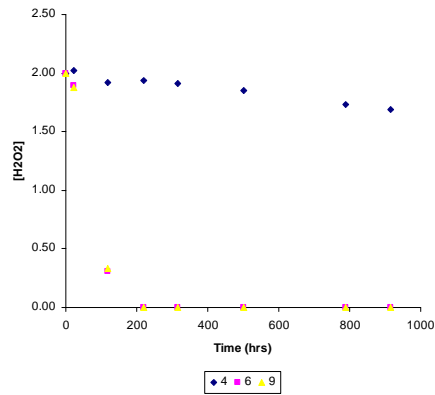
Solution Number	$t_{1/2}$ (days)	[H ₂ O ₂] (M)	[HCO ₃ ⁻] (M)	[Buffer] (μ)	[DTPA] (μM)	Misc.
1	4773	2	0	0	0	
2	30.9	2	0	0.5	0	
3	1.69	2	0.5	0	0	
4	85.2	2	0	0.5	10	
5	50.9	2	0	0.5	100	
6	1.91	2	0.5	0	10	
7	2.02	2	0.5	0	100	
8	1.95	2	0.4	0.1	0	
9	1.95	2	0.4	0.1	10	
10	2.64	2	0.4	0.1	100	0.1 M CTACl
11	4.73	2	0.4	0.1	0	0.1 M CTACl
12	4.85	2	0.4	0.1	100	4:1 v/v H ₂ O/EtOH
13	148	2	0	0	0	4:1 v/v H ₂ O/EtOH
14	324	2	0	0	100	4:1 v/v H ₂ O/EtOH
15	5.03	2	0.2	0	0	4:1 v/v H ₂ O/EtOH
16	5.79	2	0.2	0	100	4:1 v/v H ₂ O/EtOH
17	5.47	2	0.2	0.3	0	4:1 v/v H ₂ O/EtOH
18	8.46	2	0.2	0.3	100	4:1 v/v H ₂ O/EtOH
19	2.85	2	0.4	0.1	1000	
20	156	2	0	0	0	1:1 v/v H ₂ O/ Propylene Carbonate
21	15.5	2	0.5	0	0	1:1 v/v H ₂ O/ Propylene Carbonate
22	17.9	2	0.4	0.1	0	1:1 v/v H ₂ O/ Propylene Carbonate
23	165	2	0	0	1000	1:1 v/v H ₂ O/ Propylene Carbonate
24	16.5	2	0.5	0	1000	1:1 v/v H ₂ O/ Propylene Carbonate
25	15.9	2	0.4	0.1	1000	1:1 v/v H ₂ O/ Propylene Carbonate



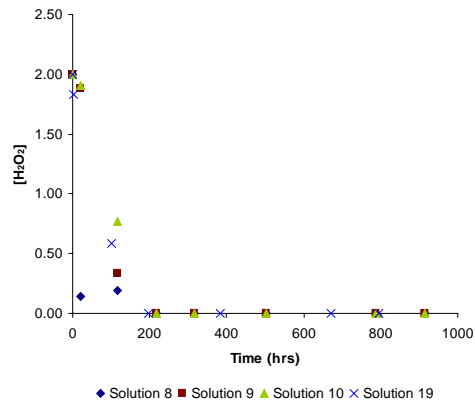
Graph 1. [H₂O₂] versus Time. Solution 4 (10 μM DTPA) Solution 5 (100 μM DTPA). Both contain: [H₂O₂] = 2M, sodium phosphate buffer = 0.5 μ, pH = 7.5.



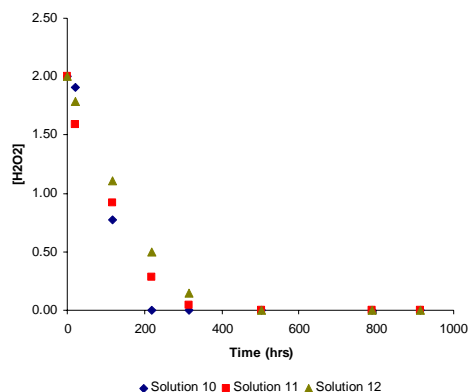
Graph 2. [H₂O₂] versus Time (hrs). Solution 2 contained: [H₂O₂] = 2 M, Buffer = 0.5 μ, pH = 7.6. Solution 4 contained: [H₂O₂] = 2 M, DTPA = 10 μM, Buffer = 0.5 μ, pH = 8.6.



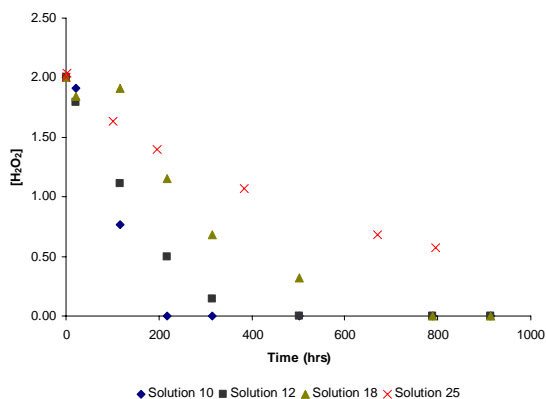
Graph 3. [H₂O₂] versus Time (hrs). Solution 4 contained: [H₂O₂] = 2 M, Buffer = 0.5 μ, DTPA = 10 μM, pH = 7.6. Solution 6 contained: [H₂O₂] = 2 M, [HCO₃⁻] = 0.5 M, DTPA = 10 μM, pH = 8.6. Solution 9 contained: [H₂O₂] = 2 M, Buffer = 0.1 μ, [HCO₃⁻] = 0.4 M, DTPA = 10 μM, pH = 8.6.



Graph 4. [H₂O₂] versus Time (hrs). All solutions contained: [H₂O₂] = 2 M, [HCO₃⁻] = 0.4 M, Buffer = 0.1 μ, pH = 8.6. DTPA concentrations: Solution 8 = 0 μM, Solution 9 = 10 μM, Solution 10 = 100 μM, Solution 19 = 1000 μM.



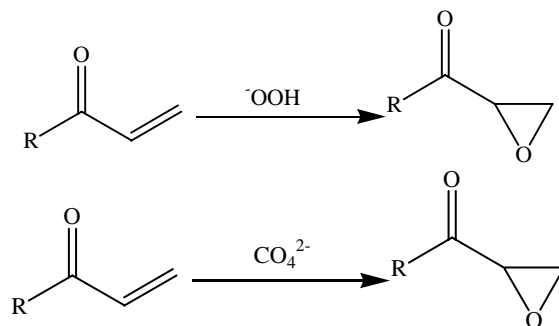
Graph 5. [H₂O₂] versus Time (hrs). Solution 10 contained: [H₂O₂] = 2 M, Buffer = 0.1 μ, [HCO₃⁻] = 0.4 M, DTPA = 100 μM, pH = 8.6. Solution 11 contained: [H₂O₂] = 2 M, [HCO₃⁻] = 0.4 M, Buffer = 0.1 μ [CTACl] = 0.1 M, pH = 8.4. Solution 12 contained: [H₂O₂] = 2 M, Buffer = 0.1 μ, [HCO₃⁻] = 0.4 M, [CTACl] = 0.1 M, DTPA = 100 μM, pH = 8.4.



Graph 6. [H₂O₂] versus Time (hrs). Solution 10 contained: [H₂O₂] = 2 M, Buffer = 0.1 μ, [HCO₃⁻] = 0.4 M, DTPA = 100 μM, pH = 8.6. Solution 12 contained: [H₂O₂] = 2 M, Buffer = 0.1 μ, [HCO₃⁻] = 0.4, [CTACl] = 0.1 M, DTPA = 100 μM, pH = 8.4. Solution 18 contained: [H₂O₂] = 2 M, [HCO₃⁻] = 0.2 M, Buffer = 0.3 μ 4:1 v/v H₂O/EtOH, pH = 8.6. Solution 25 contained: [H₂O₂] = 2 M, [HCO₃⁻] = 0.4 M, Buffer = 0.1 μ, 1:1 v/v H₂O/propylene carbonate, pH = 7.6.

VI. THE ROLE OF THE PEROXYCARBONATE DIANION IN ELECTROPHILIC ALKENE OXIDATION

We have examined the reactivity of the peroxy carbonate dianion as a nucleophilic oxidant for electrophilic substrates. We would like to compare the peroxy carbonate dianion to the hydroperoxide anion for electrophilic alkene oxidation, as seen in Scheme 1. This is important to CWA decon, since many CWA's are electrophilic substrates. We have therefore investigated the reactivity of the peroxy carbonate dianion toward electrophilic alkenes, which are convenient electrophilic models. A number of electrophilic alkenes have been employed to explore the reactivity. The reactions were monitored by the loss of the ¹H signal of the reactant and growth of the product ¹H signal in the ¹H NMR.



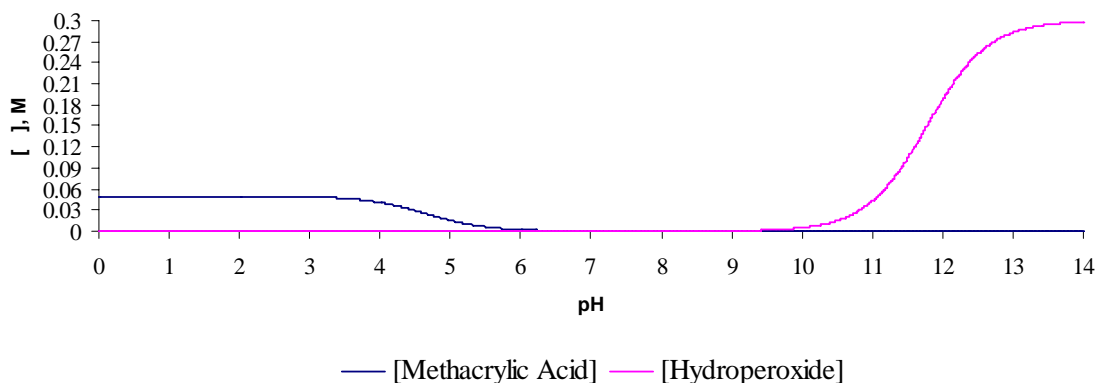
Scheme 1

The first alkene investigated was methyl vinyl ketone. Methyl vinyl ketone was oxidized with hydrogen peroxide in bicarbonate solution at pH 7.8, and a $t_{1/2}$ of 60 minutes was observed. When the pH was raised to 8.6, to allow for the equilibrium formation of more peroxydicarbonate dianion, the $t_{1/2}$ was reduced to 15 minutes. When the same experiment is conducted in sodium phosphate buffer at the identical pH using hydrogen peroxide, identical conversion to the epoxide is observed. This data are shown in Table 1. Since identical conversions to epoxide are observed in both bicarbonate and phosphate buffered solutions, this leads to the conclusion that the peroxydicarbonate dianion does not significantly contribute to electrophilic alkene oxidation over that seen for hydroperoxide alone.

Table 1- comparison of conversion of methyl vinyl ketone to epoxide in bicarbonate and phosphate buffers

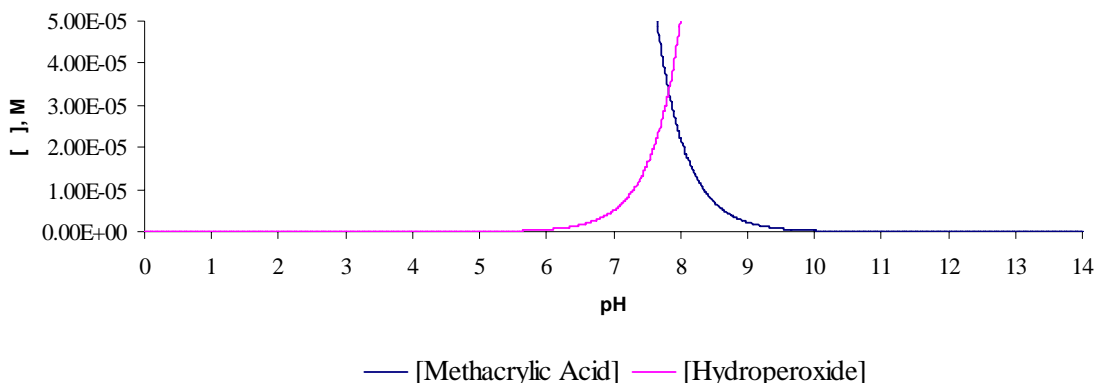
	pH 7.80, 150 min	pH 8.60, 90 min	pH 8.90, 60 min
1.0 M NaHCO ₃	74%	92%	>99%
1.0 M Na ₂ HPO ₄	74%	92%	>99%

To assure that the results are not substrate specific, oxidations of methacrylic acid were conducted under the same conditions. Methacrylic acid was oxidized with hydrogen peroxide at pH 7.8 in bicarbonate buffered solution. A 75% conversion to epoxide is observed in 24 hours. When the pH is raised to pH 8.6, only a 50% conversion to epoxide is observed in 24 hours. The reason for the decrease in oxidation at higher pH can be explained by the predominant species present at the operating pH. In order for the



Graph 3 - pH profile for [methacrylic acid] and [hydroperoxide]

oxidation to occur, the acid form of methacrylic acid will react with hydroperoxide. The pH profile for methacrylic acid and hydroperoxide concentrations are shown in Graph 3. The point where the two curves cross will be the pH at which the greatest conversion to epoxide will proceed, seen in Graph 4, a blowup of Graph 3. From the graph, that point is around pH 7.8.



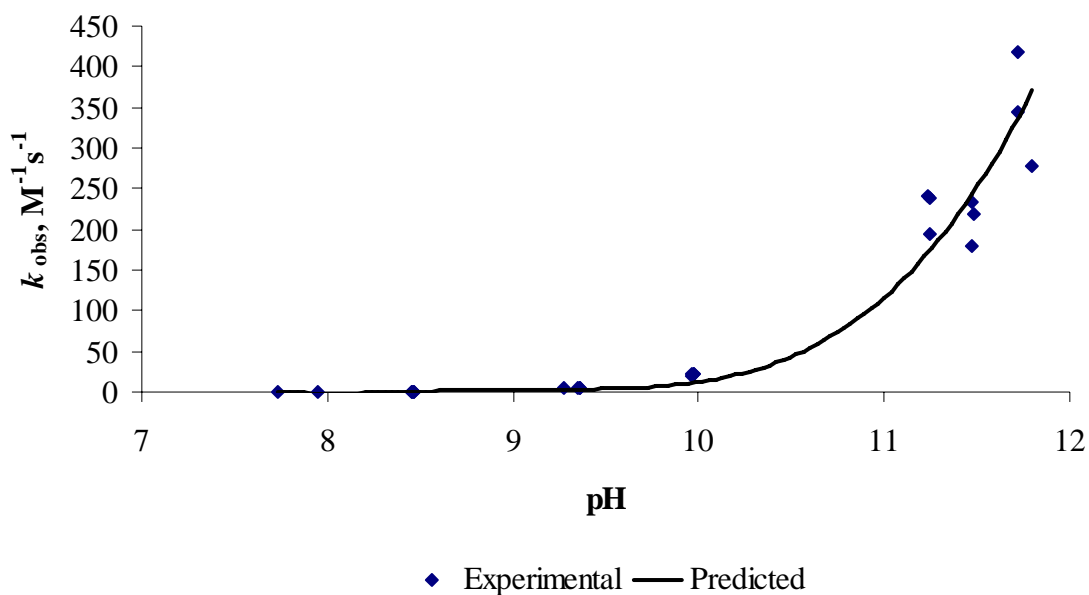
Graph 4 - Expansion of Graph 3 showing the crossing of the methacrylic acid and hydroperoxide curves

From our earlier work with nucleophilic alkene oxidation, the addition of Mn^{2+} should allow for faster conversion of methacrylic acid, since at the operating pH the acid is deprotonated. Indeed, when methacrylic acid was oxidized in bicarbonate buffer at pH 7.8 with hydrogen peroxide in the presence of $4 \mu\text{M Mn}^{2+}$, a 90% conversion to epoxide is observed in 30 minutes.

Since the acid moiety of methacrylic acid allows for the substrate to behave as a nucleophilic alkene at the operating pH, ethyl acrylate was chosen as a substrate. The acid group has been replaced by an ester, and the reactivity should return to that seen in methyl vinyl ketone oxidation. When ethyl acrylate was oxidized by hydrogen peroxide in bicarbonate buffer at pH 7.8, a 25% conversion to epoxide is observed in 24 hours. When the same reaction is conducted at the higher pH of 8.6, 66% conversion to epoxide is seen in 24 hours. The same conversions are observed for reactions in phosphate buffer at the same pH. This data supports that seen for methyl vinyl ketone oxidation. It has therefore been concluded that the peroxy carbonate dianion does not significantly contribute to electrophilic alkene oxidation compared to the background hydroperoxide oxidation.

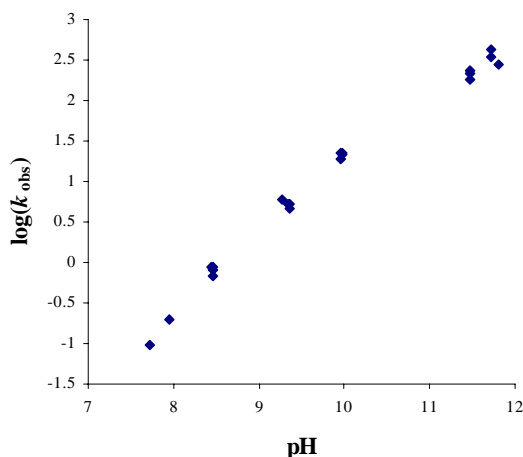
Once it was recognized that hydroperoxide was the main contributing oxidant of electrophilic alkenes, a comparative kinetic study was done between hydroperoxide and hypochlorite. Dibenzoyl ethylene was chosen as substrate for these reactions. The reaction was monitored spectrophotometrically by following the loss of absorbance of the substrate at 320 nm under second order conditions in aqueous, micellar solution.

For the reactions with hydrogen peroxide, 4.00×10^{-4} M substrate and 8.00×10^{-4} M oxidant were used. Reactions were performed in aqueous solution consisting of 0.10 M phosphate buffer and 0.10 M cetyltrimethylammonium chloride (CTACl) as surfactant. The reactions were conducted over a pH range of 7.5 – 12. A plot of the observed second order rate constant vs. pH is shown in Graph 5. The data are also



Graph 5 – Plot of k_{obs} vs. pH for oxidation with hydrogen peroxide

presented as the $\log(k_{obs})$ vs. pH in Graph 6 to show that the k_{obs} at lower pH are not in fact zero.



Graph 6 - plot of $\log(k_{obs})$ vs. pH

From this data, a rate law was derived and is shown below. The rate law indicates that there are two parameters that can be fit to the data, the rate constant and the pKa of the oxidant. Non-linear data analysis was used to provide values for the rate constant and pKa of the hydrogen peroxide oxidation of dibenzoyl ethylene. This fit to the data is presented in Graph 5. From the fit, a value of $k_1 = 660 \pm 40 M^{-1} s^{-1}$ was determined assuming that $pK_a = 11.7$.

$$v = k_1[\text{OOH}^-][\text{S}]$$

$$[\text{H}_2\text{O}_2]_0 = [\text{H}_2\text{O}_2] + [\text{OOH}^-]$$

$$K_a = \frac{[\text{OOH}^-][\text{H}^+]}{[\text{H}_2\text{O}_2]}$$

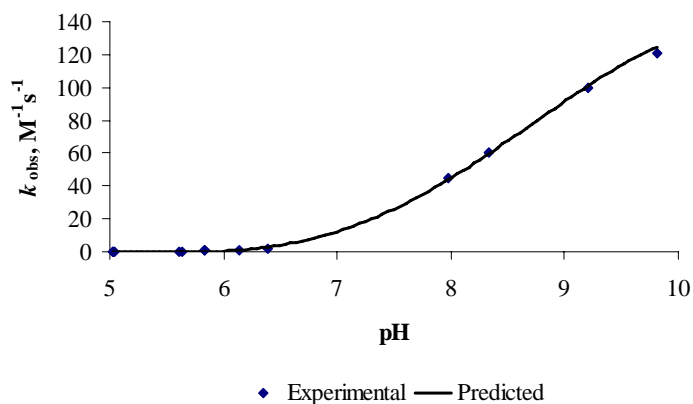
$$[\text{H}_2\text{O}_2]_0 = \frac{[\text{OOH}^-][\text{H}^+]}{K_a} + [\text{OOH}^-]$$

$$[\text{H}_2\text{O}_2]_0 = [\text{OOH}^-] \left(1 + \frac{[\text{H}^+]}{K_a}\right)$$

$$[\text{OOH}^-] = \frac{[\text{H}_2\text{O}_2]_0}{1 + \frac{[\text{H}^+]}{K_a}}$$

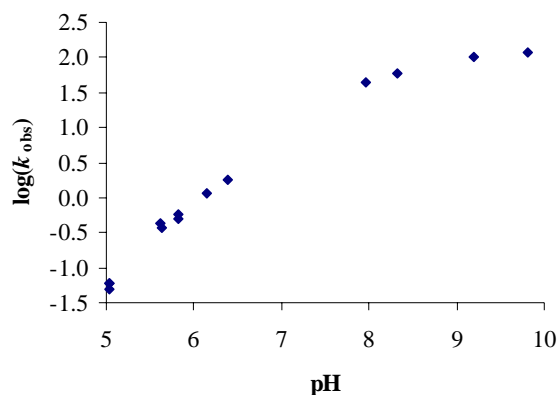
$$v = \frac{k_1[\text{H}_2\text{O}_2]_0[\text{S}]}{1 + \frac{[\text{H}^+]}{K_a}}$$

Since hypochlorite is also a nucleophilic oxidant, similar results should be found for reactions with dibenzoyl ethylene. Reaction conditions were identical to that with hydrogen peroxide, except hypochlorite concentration was 2.40×10^{-3} M and the pH range was 5 – 10. A plot of the observed second order rate



Graph 7 - plot of k_{obs} vs. pH for hypochlorite oxidation

constant vs. pH is shown in Graph 7. The corresponding log plot is shown in Graph 8. A non-linear fit to

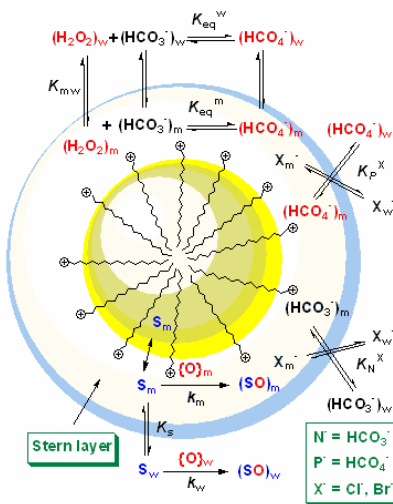


Graph 8 - log(k_{obs}) vs. pH for hypochlorite oxidation

the derived rate law is shown in Graph 7. From the fit, the value of $k_1 = 118 \pm 2 \text{ M}^{-1}\text{s}^{-1}$ and the $\text{pK}_a = 8.26$. Thus we find that OCl^- is a ca. 5-fold less reactive than OOH^- , but the reactivity of HOCl solutions in the neutral to mildly alkaline range (6 – 9) exceeds that of peroxide solutions as a result of the lower pK_a value for HOCl compared to H_2O_2 .

VII. SURFOXIDANTS

The general term *surfoxidant* has been introduced (*J. A. C. S.* **2003** 125, 6211-21) to describe the combination of an ionic surfactant with a reactive counterion that is itself an oxidant or activates an oxidant from the bulk solution to form an oxidant counterion. It was shown that the new catalytic cationic surfoxidant CTAHCO_3 (cetyltrimethyl-ammonium bicarbonate) significantly enhances the overall BAP oxidation rates for mustard simulants. In addition, we compared the surfoxidant approach to the addition of bicarbonate salts to CTACl and CTABr , where the halide counterions must undergo equilibrium displacement by the oxidant anion. General equations based on the classic pseudophase model were derived to account for the pre-equilibrium reaction in the aqueous and micellar phases, and the resulting model can be used to describe any micellar reaction with associated pre-equilibria. It was shown that the reactivity of CTAHCO_3 -activated peroxide is higher in terms of BAP oxidations compared to mixed aqueous-organic solvents.



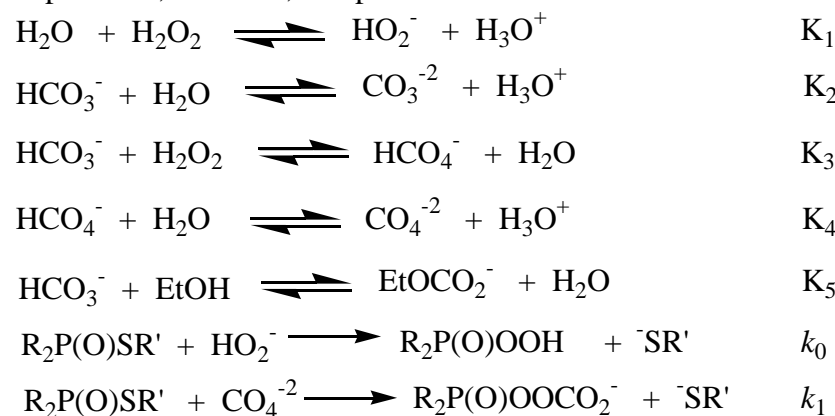
Andrew Burke and Dan Denevan continued the development of new surfoxidants. We extended the concept to surfactants combined with other reactive oxidant anions, such as hypochlorite and peracids. Their work has shown that such formulations may have enhanced stability and reactivity as found for the BAP surfoxidants.

VIII. OXIDATION AND PERHYDROLYSIS OF VX SIMULANTS BY BICARBONATE ACTIVATED PEROXIDE

Dan Denevan has investigated the nucleophilicity of BAP solutions toward organophosphorous compounds with particular emphasis on the reactivity of the peroxydicarbonate dianion (CO_4^{2-}). Peroxycarbonate has been previously investigated for oxidation of sulfides but until recently its role in the perhydrolysis of organophosphates has been unknown. Our studies targeted the kinetic and mechanistic parameters of this reaction using bicarbonate-activated peroxide. The application of BAP solutions to multiple CWA depends on its ability to oxidize and perhydrolyze agents as needed. Therefore, Denevan has investigated the kinetics of other perhydrolytic reactants, such as hypochlorite and peracids (section IX).

Simulants investigated were diphenyl phenylphosphonothioates with R groups (Cl, H, CH_3 , OCH_3 , NO_2 , CO_2H , and OH) attached in the para position of the thiolate. Previous research has shown that hydrogen peroxide can be used in the cleavage of phosphorus sulfur bond of VX by a perhydrolytic mechanism. (Yang, Szafraniec, et al. 1993) The expected pH dependence for the perhydrolytic pathway is observed. Deprotonation of H_2O_2 and HCO_3^- yields the reactive species HO_2^- and CO_4^{2-} , both of which are α -nucleophiles. Several mechanistic and kinetic parameters were investigated. We set out to determine the relative nucleophilicity of HO_2^- and CO_4^{2-} by investigating BAP perhydrolysis of several substrates, including VX simulants and traditional carboxylate esters.

The proposed mechanism for the perhydrolysis of a VX simulant is shown below, and the derived rate law is given to illustrate the complex dependence of overall rate on concentrations of peroxide, activator, and pH.



$\text{R}_2\text{P}(\text{O})\text{SR}'$ stands for the organophosphate VX simulant

Rate Law

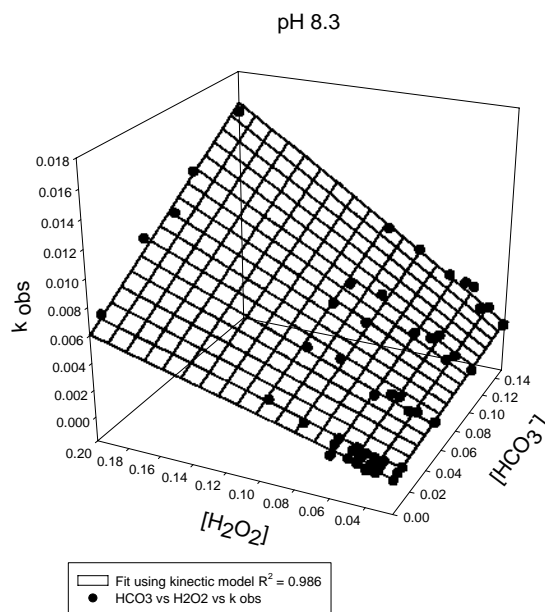
$$v = k_0 [\text{HO}_2^-][\text{R}_2\text{P}(\text{O})\text{SR}'] + k_1 [\text{CO}_4^{2-}][\text{R}_2\text{P}(\text{O})\text{SR}']$$

$$[\text{CO}_4^{-2}] = \left(\frac{K_3 K_4 [\text{H}_2\text{O}] [\text{H}_2\text{O}_2]_0 [\text{HCO}_3^-]_0}{[\text{H}_3\text{O}^+] [\text{H}_2\text{O}] + K_2 [\text{H}_2\text{O}]^2 + K_3 [\text{H}_3\text{O}^+] [\text{H}_2\text{O}_2]_0 + K_3 K_4 [\text{H}_2\text{O}] [\text{H}_2\text{O}_2]_0 + K_5 [\text{H}_3\text{O}^+] [\text{EtOH}]} \right)$$

$$-\frac{d[\text{PS}]}{dt} = k_0 [\text{OOH}^-] [\text{PS}] + k_1 [\text{CO}_4^{-2}] [\text{PS}]$$

$$[\text{HO}_2^-] = \frac{K_1 [\text{H}_2\text{O}_2]_0 [\text{H}_2\text{O}]}{K_1 [\text{H}_2\text{O}] + [\text{H}_3\text{O}^+]}$$

The kinetic parameters for the peroxide- only pathway were determined: $k_0 = 92 \pm 3 \text{ M}^{-1}\text{s}^{-1}$ and the pH dependence was well modeled by the rate law in the range $\text{pH} = 7 - 10$. Our work has focused on determination of the activation parameters, ionic strength and salt effects, solvent effects, and solvent composition effects. Activation parameters were determined by variation of the reaction temperature from 15°C to 50°C . The resulting k_{obs} values were plotted on Eyring plots (Graph 2) and ΔH^\ddagger , ΔS^\ddagger , and E_a values were obtained (Table 1). Graph 1 shows a fit of the observed rate constants to the full rate law for initial $\text{pH} 8.3$ when bicarbonate is added.



Graph 1. 3D-Plot of $[\text{HCO}_3^-]$ versus $[\text{H}_2\text{O}_2]$ versus k_{obs} . Reaction conditions: $[\text{H}_2\text{O}_2] = 0-0.20 \text{ M}$, $[\text{HCO}_3^-] = 0-0.15 \text{ M}$, $\text{pH} 8.3$ (initial), water/ethanol (4:1 v:v), $\mu = 0.15$, $\text{Ph}_2\text{P}(\text{O})\text{SPhCl}(p) = 0.5 \text{ mM}$.

The small increase in k_{obs} with increased bicarbonate (Graph 1) appears to indicate that the CO_4^{2-} pathway is enhancing the displacement of the thiol. However, close examination of the data indicates that small pH variations may be the cause of some or all of the acceleration with bicarbonate added, although ionic strength was carefully controlled and buffers were used.

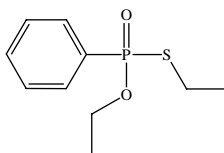
Since a mixed solvent was used (alcohol/water) in the experiments with VX simulants, we have investigated related carboxylate ester perhydrolysis in pure water to ascertain the pH effects accurately. From kinetic studies in buffered peroxide solutions, the rate constant k_0 for the reaction of OOH^- with PNPA is in agreement with the literature ($5000 \text{ M}^{-1}\text{s}^{-1}$). With phenyl acetate, the value of k_0 is $0.002 \text{ M}^{-1}\text{s}^{-1}$. The reactivity under any combination of bicarbonate and

phosphate buffer at fixed ionic strength could be described by the OOH^- reaction only and no evidence for the CO_4^{2-} pathway was found. The value of k_1 is therefore $\leq 0.002 \text{ M}^{-1}\text{s}^{-1}$ for phenyl acetate. Peroxyanions tend to be strong nucleophiles with relatively small variations in reactivity depending on chemical structure, but the hydroperoxide ion is usually the most reactive of all (section IX).

During the course of studying the VX simulants reactions it was noted that increases in the overall ionic strength decreased the rate of reaction (Graph 3). An increase in the total salt content from $\mu = 0.1$ to 0.5 decreased the observed rate by a factor of 3 in the background. Another significant observation was the effect different salts had on the observed rate. Small cations, such as Na^+ , decrease the rate while larger cations such as $(\text{CH}_3)_4\text{N}^+$ increase the rate. A discrepancy occurred with NH_4^+ where a decrease in rate compared to K^+ ion was observed. Anions had a similar trend where I^- increased the rate while Cl^- showed a decreased rate. Ion effects have been observed before and may result from solvent interactions and stabilization effects of the transition and ground states. Smaller ions such as Na^+ and Cl^- are more highly solvated while larger ions such as $(\text{CH}_3)_4\text{N}^+$ and I^- disrupt solvent interactions, such as hydrogen bonding.

Solvent composition and solvent effects were investigated to determine if various solvents or variation in the concentration of organic co-solvent affected the observed rate. Protic solvents such as methanol, isopropanol, and ethanol did show a small increase in rate compared to acetonitrile (Graph 4). This indicates that polarity of the solvents is not a contributing factor but the ability of the solvent to hydrogen bond correlates significantly with the rate.

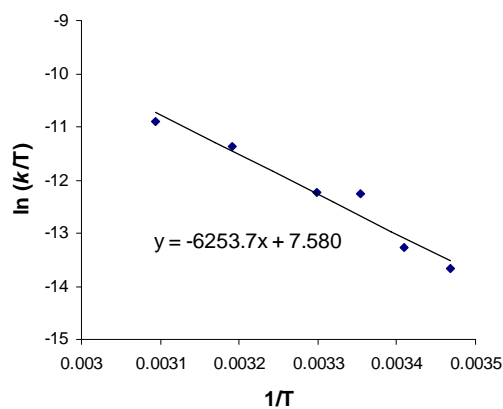
In the oxidative destruction of VX, it is highly desirable to cleave the P-S bond preferentially rather than the P-O bond. We have investigated BAP cleavage of the model substrate below, which was



O,S - diethyl phenylphosphonothioate

previously investigated in oxidative cleavage by peroxymonosulfate by Bunton and co-workers. Under all BAP conditions investigated to date, exclusive P-S cleavage has been observed by using ^{31}P -NMR. Kinetic data indicate that BAP is a more potent P-S cleavage agent than peroxide alone at a given pH and ionic strength, but the results were not definitive.

In conclusion the details of BAP reactions with VX simulants have been investigated. Variations of the reaction mixture with respect to pH, ionic strength, and temperature can significantly affect the reaction rate. Evidence for peroxymonocarbonate participation in a second perhydrolytic pathway is mixed, and the importance of such a pathway may depend on substrate. In any case, the reactivity of BAP solutions due to OOH^- is maintained compared to bicarbonate-free solutions.

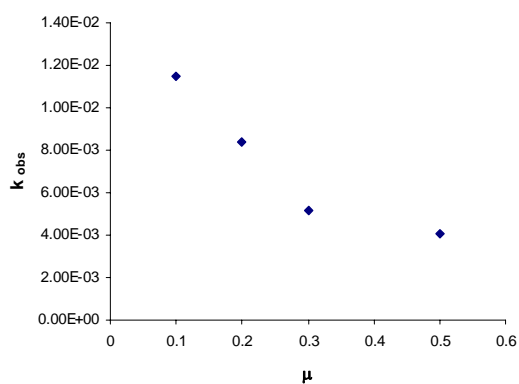


Graph 2. Eyring Plot of $\ln k_{\text{obs}}$ versus $1/T$. Reaction conditions: $[\text{H}_2\text{O}_2] = 0.01 \text{ M}$, $[\text{HCO}_3^-] = 0.01 \text{ M}$, pH 8.3, $\mu = 0.15$, water/ethanol (4:1, v:v), $T = 15.2\text{-}50 \text{ }^\circ\text{C}$, $\text{Ph}_2\text{P}(\text{O})\text{SPhCl}(p) = 0.3 \text{ mM}$.

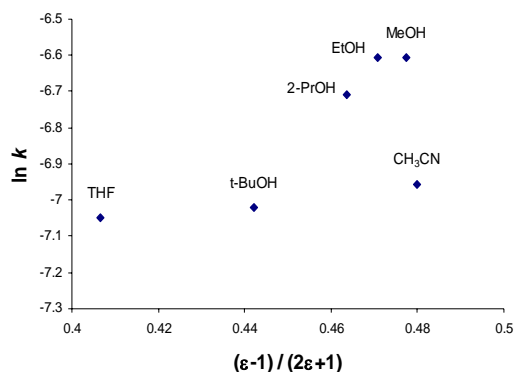
Table 1. Activation Parameters^a

Reactive Species	ΔH^\ddagger (kJ/ mol)	ΔS^\ddagger (J/ mol * K)	E_a (kJ/ mol)
OOH^-	46 ± 2	-47 ± 5	48 ± 2

^a Conditions: $[\text{H}_2\text{O}_2] = 0.01 \text{ M}$, $[\text{HCO}_3^-] = 0\text{-}0.01 \text{ M}$, $T = 15.2\text{-}50 \text{ }^\circ\text{C}$, water/ethanol (4:1, v:v), $\mu = 0.15$. The substrate was $\text{Ph}_2\text{P}(\text{O})\text{SPhCl}(p)$.



Graph 3. Plot of k_{obs} versus ionic strength (μ) with increased phosphate salts. Reaction conditions: $[\text{H}_2\text{O}_2] = 0.1 \text{ M}$, $[\text{HCO}_3^-] = 0.05 \text{ M}$, pH 8.4, water/ethanol (2.33:1, v:v), $\text{Ph}_2\text{P}(\text{O})\text{SPhCl}(p) = 0.3 \text{ mM}$



Graph 4. Plot of $\ln k$ versus $\{(\epsilon-1)/(2\epsilon+1)\}$ for the $\text{Ph}_2\text{P}(\text{O})\text{SPhCl}(p)$ reaction in several organic solvents. Reaction conditions: water/organic solvent (4:1, v:v), pH 8.3, $[\text{H}_2\text{O}_2] = 0.01 \text{ M}$, $[\text{HCO}_3^-] = 0.05 \text{ M}$, $\mu = 0.15$.

IX. PERHYDROLYSIS OF VX SIMULANTS BY HYDROPEROXIDE AND OTHER NUCLEOPHILIC REAGENTS

VX simulants are electrophilic in nature and are therefore reactive toward nucleophilic reactive ions. Results on BAP reactivity indicated that the reactive ions in this particular system are CO_4^{2-} and, primarily, HOO^- . The mechanism of the reaction typically involves attack of the nucleophilic ion (ROO^-), forming a penta-coordinate intermediate, followed by displacement of the leaving group and hydrolysis to the corresponding acid.

Both CO_4^{2-} and HOO^- are α -nucleophiles, which predicts an increased reactivity versus other nucleophiles. Nucleophilicities of the ions depend on the $\text{p}K_a$ values of the parent atom, and as the $\text{p}K_a$ increases for α -nucleophiles so does the reactivity towards electrophilic substrates. Comparing peroxy carbonate to hydrogen peroxide the corresponding $\text{p}K_a$'s are 10.6 and 11.7, indicating that hydroperoxide anion will usually have a higher reactivity with the VX simulants. Indeed, results reported by Denevan and Burke (sections VI and VIII) indicate that CO_4^{2-} does not have unusually high reactivity toward electrophiles and the reactivity of BAP solutions is dominated by hydroperoxide anion in such cases.

Solvent effects on the rates were investigated. Varying the concentration of organic solvent present in the reaction can lead to understanding on mechanism and role the solvent environment impacts on the rate. Grunwald-Weinstein plots shows $\log k$ versus Y , a quantitative measure of solvent ionizing power at specific concentrations of the solvent. Analysis of Figure 1 shows little or no dependence on solvent composition and rate as the amount of organic solvent is decreased from 50% to 10% v/v.

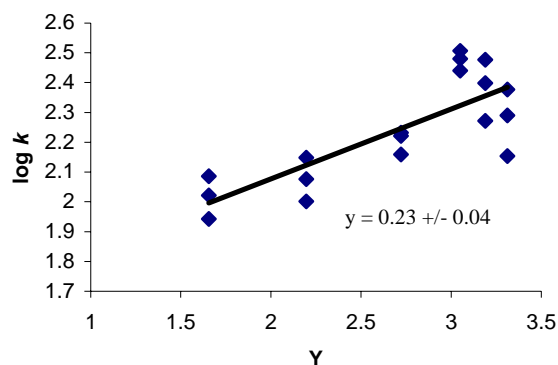


Figure 1. Grunwald – Weinstein Plot, Conditions: 0.3 mM $\text{Ph}_2\text{P}(\text{O})\text{SPhR}$, $\mu = 0.1$, $\text{pH} = 8.3\text{-}8.5$, 10-50 % $\text{EtOH}/\text{H}_2\text{O}$, 0.01 M H_2O_2

Hydrolysis of VX simulants with and without CTACl surfactant. The next step in investigating the cleavage of VX simulants was replacing the organic solvent with surfactants. Surfactants investigated were CTAX (X = OH, Cl, Br), Triton X-100, and SDS. Background reactions using CTACl were performed for the hydrolytic cleavage and perhydrolytic cleavage of $\text{Ph}_2\text{P}(\text{O})\text{SPhR}$ and $\text{Ph}_2\text{P}(\text{O})\text{OPhR}$. Eyring and Hammett correlation plots were constructed and are shown below.

A Hammett correlation plot shown below for $\text{Ph}_2\text{P}(\text{O})\text{OPhR}$ in CTACl with H_2O_2 (ρ value = 3) is similar to previous results of a positive ρ value of 1.9 ± 0.3 in 80:20 $\text{H}_2\text{O}/\text{EtOH}$ (v/v), indicating that in the presence of micelles or EtOH mixtures a similar $\text{S}_{\text{N}}2$ or addition-elimination cleavage reaction occurs.

Table 1 shows results when similar reactions are run with THF as the organic solvent instead of EtOH. This indicates that a decrease in polarity of the solvent increases ρ and not indicative of a change in solvent environment from $\text{H}_2\text{O}/\text{EtOH}$ to $\text{H}_2\text{O}/\text{CTACl}$. The micellar interior is considered nonpolar and ρ values are expected to be larger in such environments as charge buildup in the transition state is not compensated by solvation as extensively.

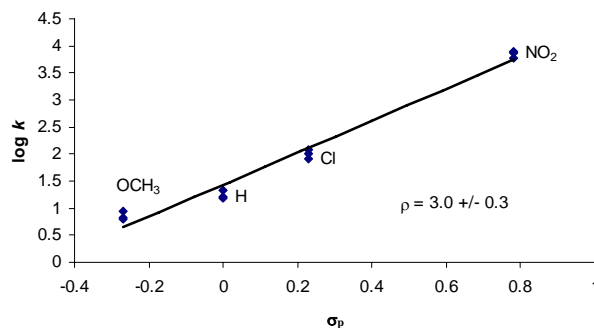


Figure 2. Hammett correlation plot. 0.3 mM $\text{Ph}_2\text{P}(\text{O})\text{OPhR}$, 0.05 M CTACl, $\mu = 0.15$, $\text{pH} = 7.9\text{-}8.0$, 0.1 M H_2O_2

Table 1. Comparison of P-S versus P-O cleavage on Hammett plots with THF as the co-solvent. 0.3 mM Simulant, 80:20 H₂O/THF, $\mu = 0.15$, pH = 8.3-8.4, 0.1 M H₂O₂.

Simulant	Ph ₂ P(O)OPhR	Ph ₂ P(O)SPhR
ρ	4.0 +/- 0.8	2.7 +/- 0.2

Activation Parameters. Second-order rate constants were used to construct an Eyring plot of $\ln(k_1/T)$ vs $1/T$, and activation parameters were derived. Using the equation $y = m * x + b$ the values are defined as:

$$\Delta H^\ddagger = -m * R$$

$$\Delta S^\ddagger = [b - 23.76] * R$$

For these experiments a temperature range of 20-50 °C or 293-323 K was investigated. The ΔH^\ddagger value for Ph₂P(O)SPhNO₂ base hydrolysis is greater than that of Ph₂P(O)OPhNO₂, as expected since the thiophenolate is a better leaving group. As seen in Figures 3 & 4 for Ph₂P(O)SPhNO₂ and Ph₂P(O)OPhNO₂ the ΔS^\ddagger has significant error and a value around 0 J/mol K. Figure 5 shows the same reaction with the exception of CTACl replacing the organic solvent. The significant difference in ΔS^\ddagger values between surfactant and homogeneous media likely arises from the distinct character of the Stern layer of a cationic surfactant. Further experiments are necessary to understand the phenomena completely. Table 2 summarizes results from the Eyring and Hammett plots.

Table 2. Values of ρ , ΔH^\ddagger , and ΔS^\ddagger for base hydrolysis and perhydrolysis of VX simulants

Exp. Type	Ph ₂ P(O)SPhR	Ph ₂ P(O)OPhR
Hammett ρ (w/ EtOH & H ₂ O ₂)	1.0 ± 0.1	1.9 ± 0.3
Hammett ρ (w/ THF & H ₂ O ₂)	2.7 ± 0.2	4.0 ± 1
Hammett ρ (w/ CTACl & H ₂ O ₂)	-	3.0 ± 0.3
Hydrolysis ΔH^\ddagger (kJ/mol)	62 ± 4	72 ± 8
Hydrolysis ΔS^\ddagger (J/mol*K)	8 ± 14	25 ± 24
Hydrolysis w/ CTACl ΔH^\ddagger (kJ/mol)	-	77 ± 0.5
Hydrolysis w/ CTACl ΔS^\ddagger (J/mol*K)	-	77 ± 15

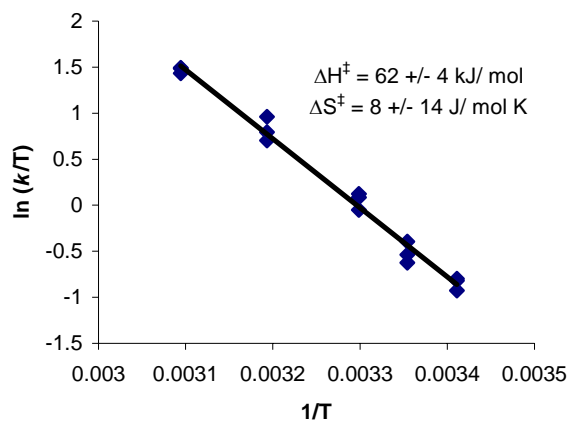


Figure 3. Eyring Plot. 0.3 mM Ph₂P(O)SPhNO₂, μ = 0.15, pH = 8.3-8.5, 80:20 H₂O/EtOH (v/v).

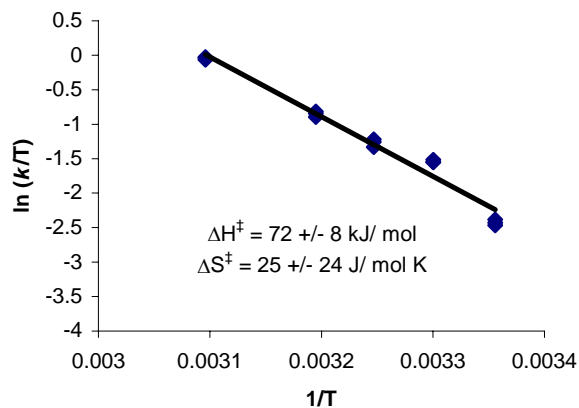


Figure 4. Eyring Plot. 0.3 mM Ph₂P(O)OPhNO₂, μ = 0.15, pH = 8.3-8.5, 80:20 H₂O/EtOH (v/v).

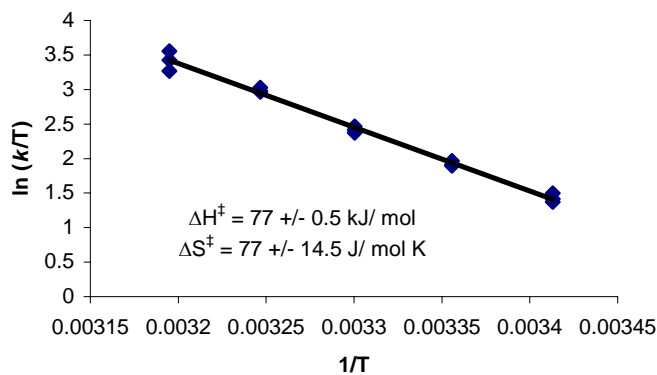
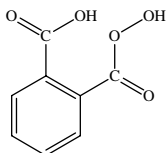


Figure 5. Eyring Plot. 0.1 mM Ph₂P(O)OPhNO₂, μ = 0.15, pH = 7.8-7.9, 0.1 M CTACl.

MMPP and mCPBA. Current investigations have focused in the development of reactive ion surfactants called surfoxidants. One example of a surfoxidant developed by this lab is CTAHCO₃, which can be mixed with hydrogen peroxide to form the reactive peroxy carbonate

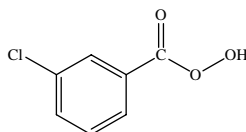
surfactant CTAHCO₄. Results show an increase in reactivity for nucleophilic substrates, such as mustard agent simulants, versus bicarbonate, hydrogen peroxide and in aqueous/organic solvent mixtures. The increased reactivity can be attributed to a localization effect of substrate and oxidant in the micellar structure. Another example from the literature is CTAOOH, where the hydroperoxide anion is micelle bound (Toullec, J.; Moukawim, M. *Chem. Commun.* **1996**, 221-222.) A new type of surfoxidants in development at UF involves replacing the counter ion of CTAOH with either magnesium monoperoxyphthalate (MMPP) or meta-chloroperoxybenzoic acid (m-CPBA).



Monoperoxyphthalate

$$pK_{a1} = 2.3$$

$$pK_{a2} = 8.2$$



m-chloroperoxybenzoic acid

$$pK_a = 7.14$$

Magnesium monoperoxyphthalate (MMPP) and *m*-chloroperoxybenzoic acid (m-CPBA) are stable organic peroxides. Both peroxides come as a solid form, and MMPP is water-soluble. As peroxides they both are able to cleave VX simulants by a nucleophilic displacement with 95% site specificity of the sulfur versus oxygen substituents of the organophosphate (EtO)(EtS)P(O)Ph. One significant disadvantage of using these peroxides is the lower pK_a's for each compared to hydrogen peroxide. Optimal reaction conditions are neutral pH with little or no organic solvent. However, at neutral pH significant proportion of the organic peroxides are deprotonated leading to significant decomposition of the organic peroxide via reaction of the anion with the neutral peroxide.

Initial studies were run in homogenous solution to determine the intrinsic reactivity of the peracid anions with paroxon. A proposed rate law is derived below for both MMPP, mCPBA and other peracids (ROOH). The pH dependence of the reactions is well modeled by the rate law. The reaction is first order for both MMPP and mCPBA, and $k_{MMPP} = 10.2 \pm 0.3 \text{ M}^{-1}\text{s}^{-1}$ and $k_{mCPBA} = 8.6 \pm 0.2 \text{ M}^{-1}\text{s}^{-1}$.

$$v = k_1[\text{ROO}^-][\text{S}]$$

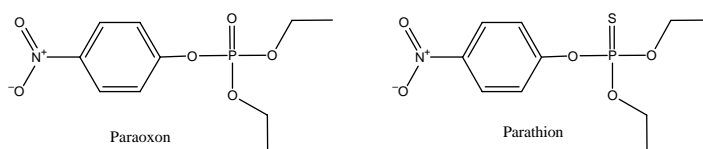
$$k_{\text{obs}} = k_1[\text{ROO}^-]$$

$$K_a = \frac{[\text{ROO}^-][\text{H}^+]}{[\text{ROOH}]}$$

$$[\text{ROO}^-] = \frac{K_a[\text{ROOH}]_0}{K_a + [\text{H}^+]}$$

$$k_{\text{obs}} = \frac{k_1 K_a [\text{ROOH}]_0}{K_a + [\text{H}^+]}$$

Paraoxon and parathion syntheses. Improved syntheses of two commonly used organophosphate CWA simulants were developed. Syntheses of paraoxon ((EtO)₂P(O)OPhNO₂) and parathion ((EtO)₂P(S)OPhNO₂) were accomplished by using the potassium salt of the nitrophenol with either diethyl chlorophosphate or diethyl chlorothiophosphate in dry benzene. The mixture was refluxed in a Dean Stark apparatus for two to three days and cooled using an ice-water bath. The precipitate of potassium chloride was filtered off. The organic solution was washed with chilled solution 3x30 ml of 0.1 M KOH/ 0.1 KCl mixtures and a separate wash of 3x30 mL of chilled H₂O. The solution was washed again with 20 ml H₂O or until no yellow or orange color was observed in the water layer. Using anhydrous sodium sulfate the organic layer was dried for 30 min and the sodium sulfate was filtered off. Benzene was removed under reduced pressure resulting in a light yellowish oil for paraoxon and a slightly orange oil for parathion. Yields were 4.91 g, 90% for paraoxon and 4.3 g, 78% for parathion. Paraoxon ¹H NMR (CDCl₃): δ 8.23 (d, J = 9 Hz, 2 H), 7.38 (d, J = 9.3 Hz, 2 H), 4.24 (q5, 4 H), 1.36 (t, 6H) ³¹P: δ -5.401 (s). Parathion ¹H NMR (CDCl₃): δ 8.19 (d, 2 H), 7.31 (d, 2 H), 4.22 (m, 4 H), 1.33 (t, 6H) ³¹P: δ 62.8 (s).



Variation of peroxide types for perhydrolytic cleavage of paraoxon. Various peroxides were examined to determine if one was more effective for the perhydrolytic cleavage of paraoxon than others. Peroxides included in the study were t-butyl hydroperoxide, cumene hydroperoxide, peracetic acid, and hydrogen peroxide.

Table 3 summarizes the kinetics for the perhydrolytic cleavage of paraoxon. Peracetic acid appears to have a significant observed rate enhancement other peroxides studied, but using a similar rate law proposed for MMPP and m-CPBA anions, the actual second order rate constant for hydroperoxide anion is approximately 60 times greater than that of the peracetic acid anion. This would be expected if both the anion of peracetic acid and hydrogen peroxide act as α -nucleophiles. The pK_a of peracetic acid is 8.1 and 11.78 for hydrogen peroxide and follows the trend observed before - a higher pK_a translates to higher reactivity of the α -nucleophile.

Table 3. Observed and calculated rate constants for various peroxides in the cleavage of paraoxon.

Reactive species	pH	$10^{-6} \times k_{\text{obs}} (\text{s}^{-1})$	$k_1 (\text{M}^{-1}\text{s}^{-1})$
Hydroxide ion (OH ⁻)	8.6	2.0	0.66
Peracetic acid (CH ₃ C(O)OO ⁻)	7.3	36	0.026 ± 0.002
Hydrogen Peroxide (HOO ⁻)	8.7	13	1.6 ± 0.05
t-Butyl hydroperoxide ((CH ₃) ₃ COO ⁻)	8.7	1.9	0.96
Cumene hydroperoxide ((C ₆ H ₅)C(CH ₃) ₂ OO ⁻)	8.7	1.8	0.58

All reactions run with 1mM paraoxon, 80:20 H₂O/EtOH (v/v), $\mu = 0.15$ PB, 10 mM ROOH. PB = phosphate buffer of K₂HPO₄ and KH₂PO₄. k_1 is corrected for [ROOH] anion

Table 4 summarizes results for identical reaction conditions to Table 3 except the organic solvent, ethanol, is replaced by the surfactant CTACl. Again the observed rate constant for peracetic acid is higher than other peroxides. Using the same scheme as above, the rate constant for hydroperoxide anion was greater than peracetic acid anion. In general, all the other peracids have similar efficacy in these simulat cleavage reactions.

Table 4. Observed and calculated rate constants for various peroxides in the cleavage of paraoxon in CTACl

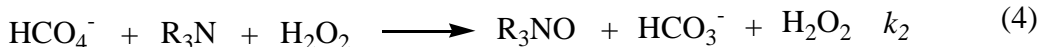
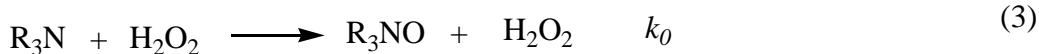
Reactive species	pH	$10^{-6} \times k_{\text{obs}} (\text{s}^{-1})$	$k_1 (\text{M}^{-1}\text{s}^{-1})$
Hydroxide ion (OH^-)	7.8	10	17
Peracetic acid ($\text{CH}_3\text{C}(\text{O})\text{OO}^-$)	6.6	300	0.98 ± 0.01
Hydrogen Peroxide (HOO^-)	7.8	29	26.7 ± 0.2
t-Butyl hydroperoxide ($(\text{CH}_3)_3\text{COO}^-$)	7.8	9.7	39
Cumene hydroperoxide ($(\text{C}_6\text{H}_6)\text{C}(\text{CH}_3)_2\text{OO}^-$)	7.8	9.3	22

All reactions run with 1mM paraoxon, 80:20 $\text{H}_2\text{O}/\text{EtOH}$ (v/v), $\mu = 0.15$ PB, 10 mM ROOH, 0.1 M CTACl
PB = phosphate buffer of K_2HPO_4 and KH_2PO_4 . k_1 is corrected for $[\text{ROOH}]$ anion

X. N-OXIDATION OF TERTIARY AMINES BY PEROXYMONOCARBONATE: KINETIC AND MECHANISTIC STUDIES

In acidic solution, the nitrogen in VX is protonated and not oxidized, whereas in basic and neutral solutions commonly employed in decontaminant formulations, the tertiary amine moiety is oxidized to the stable N-oxide more rapidly than the sulfur is oxidized. This rapid reaction can be attributed to the higher nucleophilicity of nitrogen atom compared to sulfur in VX. In the situation where only the nitrogen is oxidized for lack of either sufficient oxidant or a sufficiently strong oxidant to attack the sulfur, VX is not detoxified because the N-oxide product is still toxic.

Mechanism. To improve our understanding of amine oxidations in the chemical warfare agent VX under basic and neutral conditions, we further investigated the reactivity of BAP in tertiary amine oxidation. We have taken N-methyl morpholine as a model substrate for the kinetic and mechanistic studies of amine oxidation. The proposed mechanism is essentially identical to that used to model sulfide oxidations (below and Figure 1) at pH values well below the pKa of hydrogen peroxide. Peroxymonocarbonate is formed from bicarbonate and hydrogen peroxide (eq 1) and subsequently oxidizes the amine to amine oxide (eq 2). The kinetic behavior of the catalytic reaction conforms to the rate law of eq 5, which is derived for eqs 1-3 and takes into account the protonation of the amine at the reaction pH.



$$\frac{-d[\text{R}_3\text{NO}]}{dt} = \frac{k_1[\text{HCO}_3^-] K_{eq} [\text{H}_2\text{O}_2] A_f [\text{A}]_t}{1 + K_{eq} [\text{H}_2\text{O}_2]} + k_0 A_f [\text{H}_2\text{O}_2] [\text{A}]_t \quad (5)$$

$$= k_{obs} [\text{H}_2\text{O}_2] [\text{A}]_t \quad (6)$$

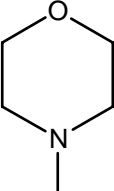
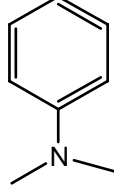
$$k_{obs} = \frac{k_1 K_{eq} [\text{HCO}_3^-] A_f}{1 + K_{eq} [\text{H}_2\text{O}_2]} + k_0 A_f$$

$$A_f = \frac{\text{Fraction of unprotonated amine}}{K_a + [\text{H}^+]} = \frac{K_a}{K_a + [\text{H}^+]}$$

The oxidation of nucleophiles by HCO_4^- has been suggested to proceed by two pathways as in Figure 1. As we are studying the reaction rates at low $[\text{H}_2\text{O}_2]$, the k_2 path has been neglected and the eq 4 is not included in the rate law. Therefore the catalytic rate constants k_1 were determined for tertiary amines in this work by substituting known values for the relevant equilibrium constants K_a and the observed rate constants into eq 5. The values for k_1 along with the background rate constants k_0 for two tertiary amines are given in Table 1. Rate constants for oxidation by peroxymonocarbonate were found to be 400-450 times greater than those for the direct reaction with H_2O_2 , and this result is consistent with previous observations for sulfides. The rate constants are comparable to those for sulfides (HD simulants) but are far higher than those for direct oxidation of the P-S bond in VX. The activity of BAP for various other tertiary and secondary amines has also been examined (Tables 2,3).

We also have investigated the oxidation reaction using CO_2 and H_2O_2 as catalysts (Table 4). The reaction profile is consistent with the formation of peroxymonocarbonate species via perhydration of CO_2 by H_2O_2 followed by deprotonation in the presence of basic substrates such as amines.

Table 1. Kinetic Parameters for Amine Oxidations by Bicarbonate-Activated Hydrogen Peroxide^a

Substrate	$10^3 k_0/\text{M}^{-1}\text{S}^{-1\text{b}}$	$k_1/\text{M}^{-1}\text{S}^{-1}$	k_1/k_0
	0.04 ± 0.003	0.016 ± 0.001	457
	0.1 ± 0.007	0.042 ± 0.002	409

^a Conditions: 25C, $[\text{H}_2\text{O}_2] = 0.5 \text{ M}$, $[\text{HCO}_3^-] = 0.5 \text{ M}$. The k_1 values were derived from k_{obs} values and eq 5 (with correction for the background reactions) assuming $k_2[\text{H}_2\text{O}_2]$ is negligible.^b k_0 is the second-order rate constant for the background reaction $\text{RNR}'\text{R}'' + \text{H}_2\text{O}_2 \rightarrow \text{RN}(\text{O})\text{R}'\text{R}'' + \text{H}_2\text{O}$. k_1 and k_0 values are derived from fitting of the data using SigmaPlot. Errors shown are quoted as standard errors.

Figure 1. Proposed mechanism for the BAP catalyzed N-oxidation reaction

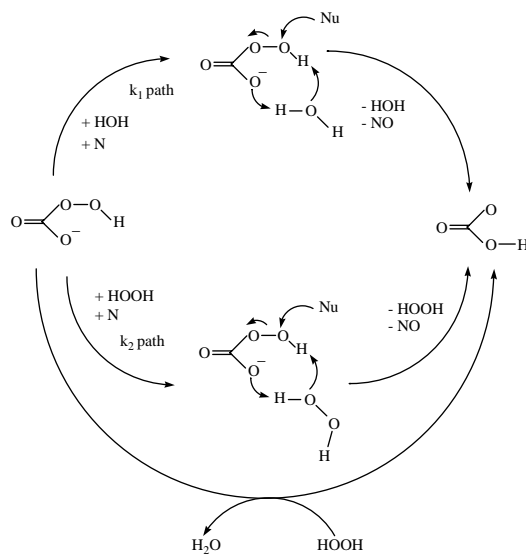


Table 2. Activity of BAP for N- oxidation of tertiary amines^a

Bicarbonate	Substrate	Time/m in	N-oxide % Yield (NMR)	pH	pKa ^c
(NH ₄)HCO ₃	N-methyl morpholine	10	35.9	8.78	7.4
NaHCO ₃		15	47.2		
		30	67.0		
			92.5 ^b		
			91.4 ^b		
	10	35.9	8.53		
	15	47.6			
	30	66.6			
(NH ₄)HCO ₃	N,N-dimethyloctylamine	15	31.1	9.56	9.86
NaHCO ₃		30	51.4		
		60	72.9		
			89.3 ^b		
			91.0 ^b		
	20	36	9.47		
	30	49.2			
	60	71.2			
(NH ₄)HCO ₃	N,N-dimethylbenzylamine	10	25.4	9.08	8.8
NaHCO ₃		15	33.3		
		30	47.9		
		240	98.9		
			90.2 ^b		
			92.1 ^b		
	15	37.1	9.16		
	30	43.1			
	60	60.3			
(NH ₄)HCO ₃	N,N- dimethylcyclohexylamine	15	29.8	9.04	10.72
NaHCO ₃		30	34.8		
		60	53.5		
		120	71.6		
(NH ₄)HCO ₃	Triethylamine	15	12.9	9.05	10.75
NaHCO ₃		30	24.5		
		60	31.7		
		120	42.0		

^a Conditions: [A] = 0.05 M, [H₂O₂] = 0.5 M, [HCO₃⁻] = 0.25 M, T = 25 °C, ^b Isolated yield ^c pKa of substrate

Table 3. Activity of BAP for oxidation of secondary amines^a

Bicarbonate	Substrate	Time/h	Nitron/ %Yield (NMR)	pH	pKa
(NH ₄)HCO ₃	Dibutylamine	3 16	74 92	10.2	11.03±0.2
(NH ₄)HCO ₃	Dibenzylamine	4	94	10.34	8.76±0.2
(NH ₄)HCO ₃	Diisopropylamine	24	34	10.21	10.76±0.2

^aConditions: [A] = 0.05 M, [H₂O₂] = 0.5 M, [HCO₃⁻] = 0.25 M, T = 25 °C, ^bpKa of substrate

Table 4. NMM Oxidation using CO₂ and H₂O₂^a

[Amine]:[H ₂ O ₂] /eqv	Period of CO ₂ flushing	[HCO ₃ ⁻] /eqv	Time/h	%Yield (NMR)	pH	~ t _{1/2}
1 : 5	1h	0	2.0	100	6.87	> 15 min
1 : 1.5	10min	0	0.5	23.8	7.07	2h
			1.0	40		
			2.0	52.9		
			3.0	64.3		
1 : 2	10min	0	1	37	7.27	2h
			2	53		
1 : 2	5min	0	1.0	52.3	7.36	1h
1 : 2	0	1	0.5	56	7.57	20min
			1.0	81.3		

^aConditions: [A] = 0.25 M, [H₂O₂] = 0.25-1.5 M, [HCO₃⁻] = 0-0.25 M, T = 25 °C,

pH Dependence. We have examined the pH dependence of the oxidation of N-methyl morpholine in detail (Figure 2). Studies on the pH dependence of rate constants by using phosphate buffers showed that changes in the kinetic constants are negligible within the experimental error in the pH range of 8-9. Above pH 9 and below pH 8, the catalytic rate does decline significantly. This decreased oxidation rates resulted from the deprotonation of HCO₃⁻ to form CO₃²⁻ at pH >9, which presumably is a less electrophilic oxidant, and the protonation of amine at pH <8. The pH region 8-9 is predicted from the relevant pKa values to be the maximum.

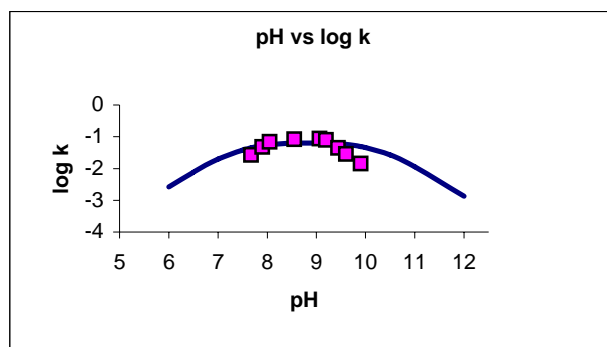
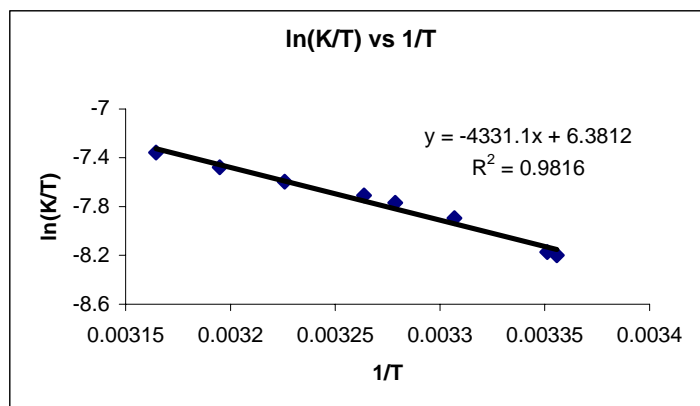


Figure 2 ■: Observed rate constants for bicarbonate catalyzed reaction $[\text{HCO}_3^-] = 0.25\text{M}$, $[\text{H}_2\text{O}_2] = 0.5\text{M}$, Solid line: Calculated rate constant from rate law

Activation Parameters for N-methyl morpholine oxidation. The temperature dependence of the catalytic NMM oxidation from 25 to 45 °C was studied in water with 0.5 M H_2O_2 and up to 0.5 M bicarbonate. The second-order rate constant (after correction for background oxidation) was used to construct an Eyring plot of $\ln(k_1/T)$ vs $1/T$, and activation parameters were derived. From a regression analysis, $H^\ddagger = 36 \pm 5 \text{ kJ mol}^{-1}$ and $S^\ddagger = -144 \pm 16 \text{ J mol}^{-1} \text{ K}^{-1}$ (errors are standard errors, $N = 8$). An Eyring analysis of the background data for direct H_2O_2 oxidation led to $H^\ddagger = 68 \pm 5 \text{ kJ mol}^{-1}$ and $S^\ddagger = -67 \pm 17 \text{ J mol}^{-1} \text{ K}^{-1}$. These values are consistent with a bimolecular reaction between neutral amines and the HCO_4^- oxidant.

Figure 3. Eyring plot for BAP catalyzed NMM oxidation



^a Conditions: $[\text{A}] = 0.05 \text{ M}$, $[\text{H}_2\text{O}_2] = 0.5 \text{ M}$, $[\text{HCO}_3^-] = 0.25 \text{ M}$, $T = 25.4\text{-}43 \text{ °C}$. Errors shown are quoted as standard errors. The substrate is N-methyl morpholine .

XI. BIOLOGICAL IMPLICATIONS OF BAP CHEMISTRY: AMINO ACID, PROTEIN, AND DNA OXIDATION

Kinetic and thermodynamic evidence was reported for the role of the peroxydicarbonate ion, HCO_4^- , as a reactive oxygen species in biology (*FRBM*, 2003, 35, 1538-50) .

Peroxydicarbonate results from the equilibrium reaction of hydrogen peroxide with bicarbonate via the perhydration of CO_2 . The oxidation of methionine by bicarbonate-activated peroxide is catalyzed by the carbonic anhydrase model compound 1,4,7,10-tetraazacyclododecanzinc(II), which accelerates the dehydration of bicarbonate and the

formation of HCO_4^- . The kinetic parameters for HCO_4^- oxidation of free methionine have been obtained ($k_c = 0.5 \pm 0.1 \text{ M}^{-1}\text{s}^{-1}$). At the physiological concentration of bicarbonate in blood (~25 mM), it is estimated that peroxymonocarbonate formed in equilibrium with hydrogen peroxide will oxidize methionine approximately two-fold more rapidly than plasma H_2O_2 itself. As an example of methionine oxidation in proteins, the bicarbonate-catalyzed hydrogen peroxide oxidation of $\alpha 1$ -proteinase inhibitor ($\alpha 1$ -PI) has been investigated via its inhibitory effect on porcine pancreatic elastase activity. The second-order rate constant for HCO_4^- oxidation of $\alpha 1$ -PI ($0.36 \pm 0.06 \text{ M}^{-1}\text{s}^{-1}$) is comparable to that of free methionine, suggesting that methionine oxidation is occurring. Further evidence for methionine oxidation, specifically involving Met358 and Met351 of the $\alpha 1$ -PI reactive center loop, has been obtained through amino acid analyses and mass spectroscopic analyses of proteolytic digests of the oxidized $\alpha 1$ -PI. These results strongly suggest that HCO_4^- should be considered a reactive oxygen species in aerobic metabolism.

In submitted work, the effect of bicarbonate on the rates of the H_2O_2 oxidation of cysteine, glutathione, and *N*-acetylcysteine to the corresponding disulfides was investigated. The relative oxidation rates at pH 8 for the different thiols are inversely related to the pK_a values of the thiol groups, and the reactive nucleophiles are identified as the thiolate anions or their kinetic equivalents. The estimated second-order rate constants at 25° C for the reaction of the thiolate anions with hydrogen peroxide are $17 \pm 2 \text{ M}^{-1} \text{ s}^{-1}$ for all three substrates. In the presence of bicarbonate (>25 mM), the observed rate of thiolate oxidation is increased by a factor of two or more, and the catalysis is proposed to be associated with the formation of peroxymonocarbonate from the equilibrium reaction of hydrogen peroxide with bicarbonate (via CO_2). The calculated second-order rate constants for the direct reaction of the three thiolate anions with peroxymonocarbonate fall within the range of 900 to 2000 $\text{M}^{-1}\text{s}^{-1}$. Further oxidation of disulfides by peroxymonocarbonate results in the formation of thiosulfonate and sulfonate products. These results strongly suggest that peroxymonocarbonate should be considered a reactive oxygen species in aerobic metabolism with relevance in thiol oxidations.

Daniel Morgan has shown that $\text{Cu}(2+)$ is a more potent activator for BAP oxidation chemistry than $\text{Mn}(2+)$ in reactions with DNA. In particular, $\text{Cu}(2+)$ strongly catalyzes the Fenton-like cleavage of DNA strands in the presence of bicarbonate. This result may suggest alternative formulations for biological decontamination. We are currently at the very early stages of understanding the Cu catalysis, but it clearly has a different mechanism than that of Mn.

XII. USE OF BAP AS AN ACTIVATOR FOR MN CATALYSTS

Our experience with $\text{Mn}(2+)$ catalyzed BAP oxidations suggested that BAP may be a general reagent for oxidations catalyzed by other metal complexes commonly used in conjunction with reactive peracids. A few examples of metal catalysts have been investigated by Ana Ison, including water soluble Mn porphyrins. Although oxidations proceed rapidly (for example, epoxidations) with BAP conditions, we have determined that such catalysts are rapidly bleached, releasing free Mn ions, and the ultimate reactivity is no different from that of $\text{Mn}(2+)$ enhanced BAP. It has also been shown that $\text{Mn}(2+)$ enhanced BAP is an oxidant for C-H bonds in water soluble organics. Therefore, in view of the instability of organic components, we conclude that ligand supported Mn is not generally superior to free Mn for many chemical oxidations. Burke has shown that a prominent study of MnL catalyzed peroxidations in the literature is actually the chemistry of the free Mn/bicarbonate system following rapid ligand degradation.

XIII. PRELIMINARY STUDIES ON PORTABLE CHLORINE DIOXIDE GENERATORS

Given the uncertain stability of peroxide as an oxidant, we have briefly investigated methods for incorporating high concentration ClO_2 generation into a portable sprayer assembly. Working prototypes have been constructed using our technology. Generation of ClO_2 is based on either acid disproportionation of chlorite or, preferably, on its one electron oxidation. Both methods have potential to produce very high concentrations of ClO_2 .